X-ray Diagnostics*

Presentation to:

2008 Warm Dense Matter Winter School

January 10 - 16, 2008

Lawrence Berkeley National Laboratory

Berkeley, California, USA

Siegfried H. Glenzer

Lawrence Livermore National Laboratory (USA)

*** This work performed under the auspices of the U.S. Department of Energy by Lawrence Livermore National Laboratory under Contract DE-AC52-07NA27344. Also supported by LDRDs 08-ERI-002, 08-LW-004, SEGRF SFB162, the Alexander-von-Humboldt foundation and the National Laboratory User Facility program.**

Collaborators

OL Landen, P Neumayer, T Döppner, RW Lee, A Ng, D Price, FJ Rogers, S Weber, R Wallace
Lawrence Livermore National Laboratory (USA)*

HJ Lee, A Kritcher, E. Morse, R Falcone
UC Berkeley (USA)

SP Regan, D Meyerhofer
Laboratory for Laser Energetics (USA)

N. Kugland, C Constantin, C. Niemann
University of California Los Angeles (USA)

G Gregori
Rutherford Appleton Laboratory (UK)

K Wünsch, D O Gericke
University of Warwick (UK)

C Fortmann, V Schwarz, R Redmer
University of Rostock (Germany)

*** This work performed under the auspices of the U.S. Department of Energy by Lawrence Livermore National Laboratory under Contract DE-AC52-07NA27344. Also supported by LDRDs 08-ERI-002, 08-LW-004, SEGRF, SFB162, the Alexander-von-Humboldt foundation and the National Laboratory User Facility program.**

Accurate diagnostics of the physics of Warm Dense Matter has been developed applying X-ray Thomson scattering

- Introduction
  - X-ray Thomson scattering from solid density plasmas
- Proof of principle experiments
  - Backscattering experiment
    - Compton scattering in dense plasmas
    - Accurate temperature diagnostics
  - Forward scattering experiment
    - First observation of Plasmons in Warm Dense Matter
    - Accurate density diagnostic
    - Importance of collisions
- Compressed Matter
  - Compressibility and adiabat
  - Structure Factors
  - Coalescing shocks
- Outlook and Conclusions


Livermore, California - 45 min from Berkeley
LLNL
NIF-0605-10997-L2
P9266


San Francisco
Berkeley
LLNL
National Ignition Facility
NIF-0605-10997-L28
P9292

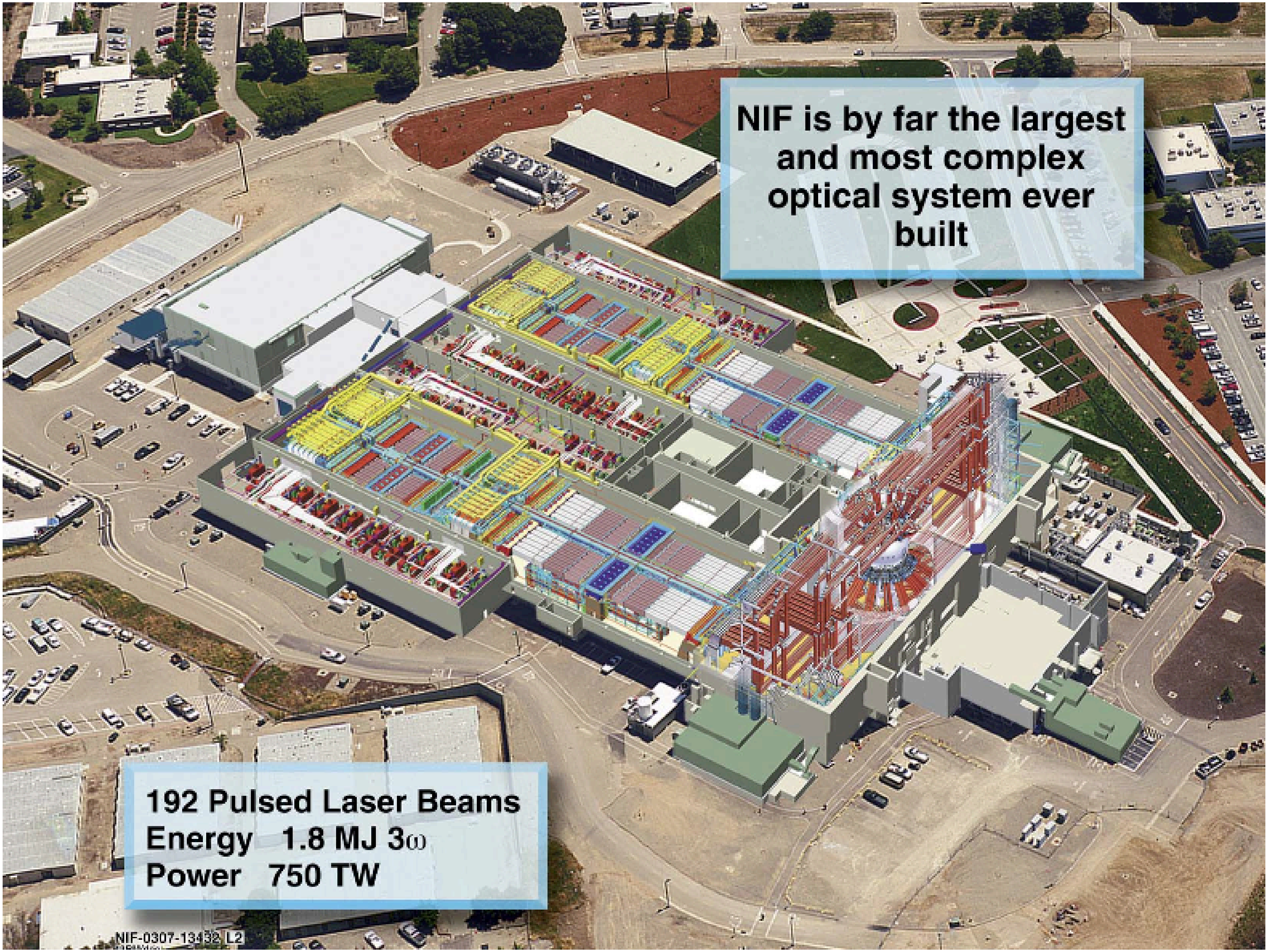
NIF is by far the largest and most complex optical system ever built
192 Pulsed Laser Beams
Energy 1.8 MJ 3ω
Power 750 TW
NIF-0307-13432 L2

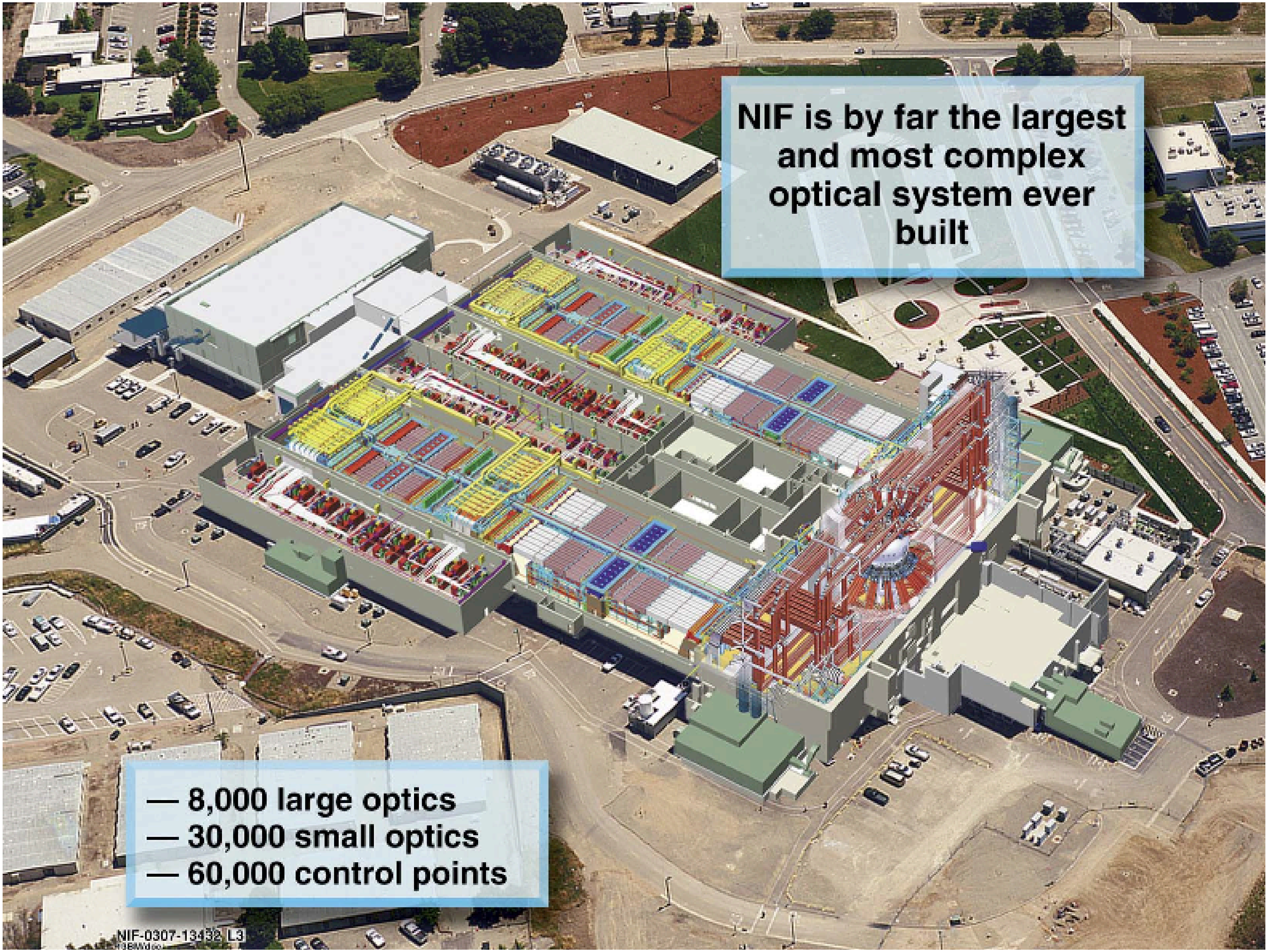
NIF is by far the largest and most complex optical system ever built
— 8,000 large optics
— 30,000 small optics
— 60,000 control points
NIF-0307-13432 L3

6,206 line replaceable units (LRUs) are being assembled, installed, and commissioned to complete NIF

The National Ignition Campaign

Preamplifier Modules (48)

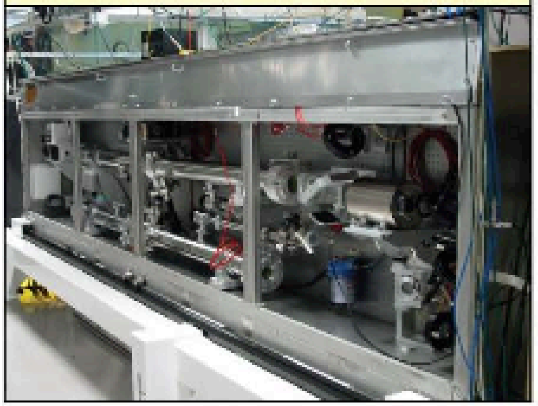

Laser Amplifiers (672)

Final Optics Assemblies (960)

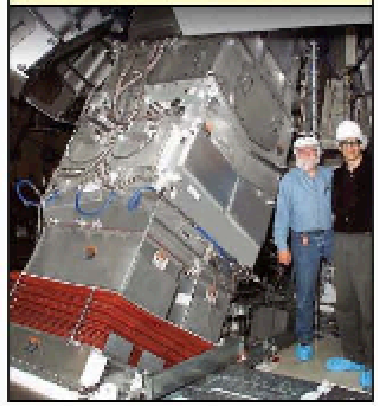

Laser Mirrors (656)

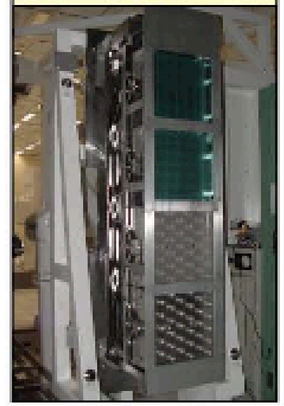

Spatial Filter Lenses (960)

Spatial Filter Towers (72)

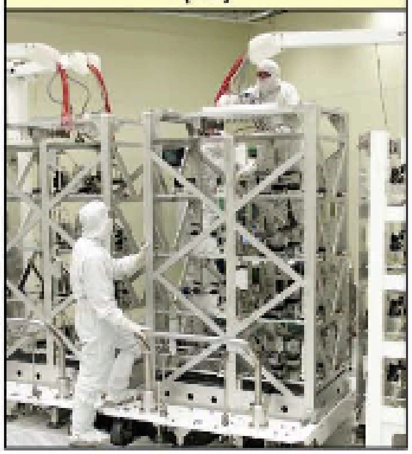

Plasma Electrode Pockels Cell (48)

Flashlamps (1008)

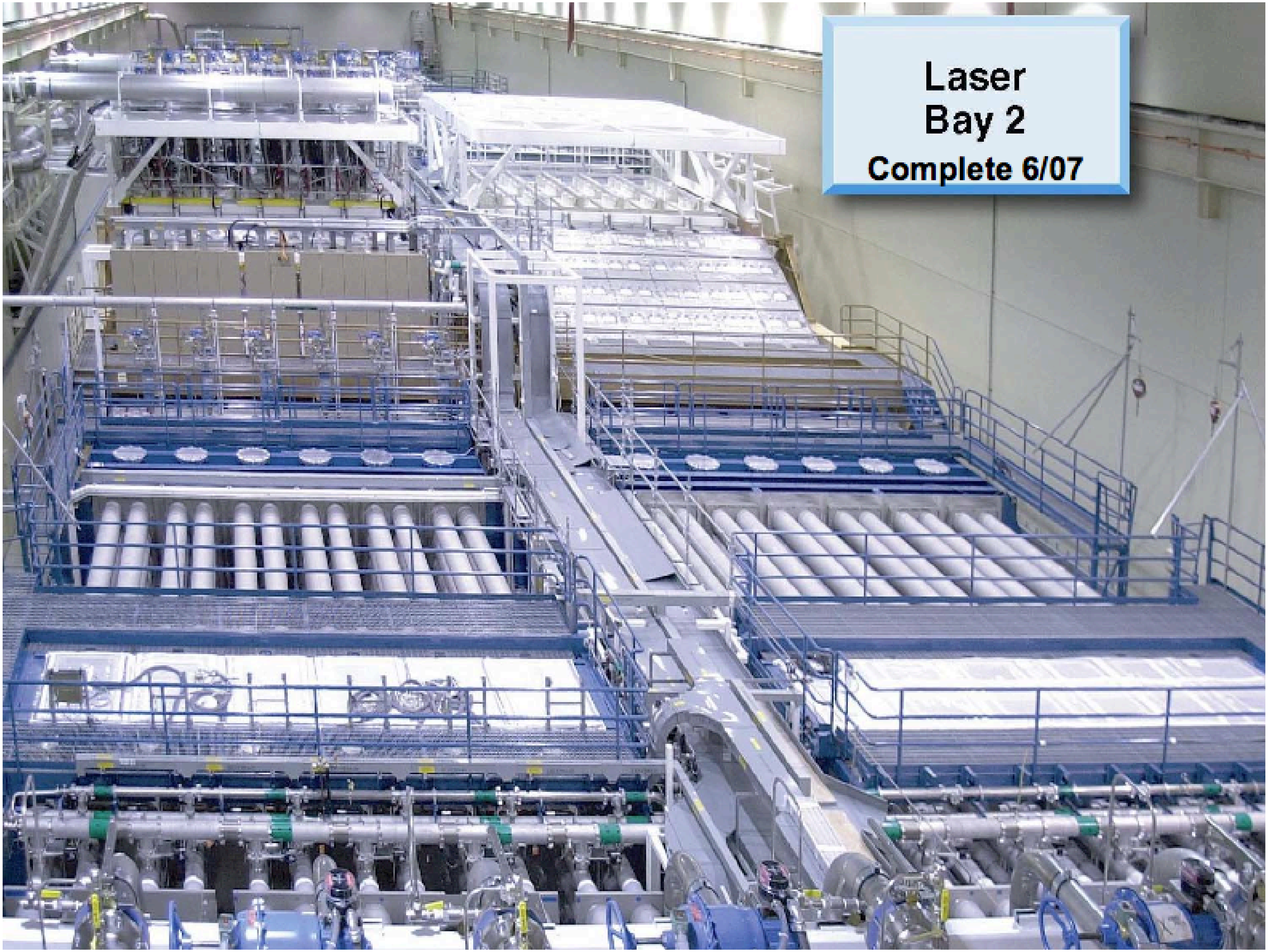
Laser
Bay 2
Complete 6/07

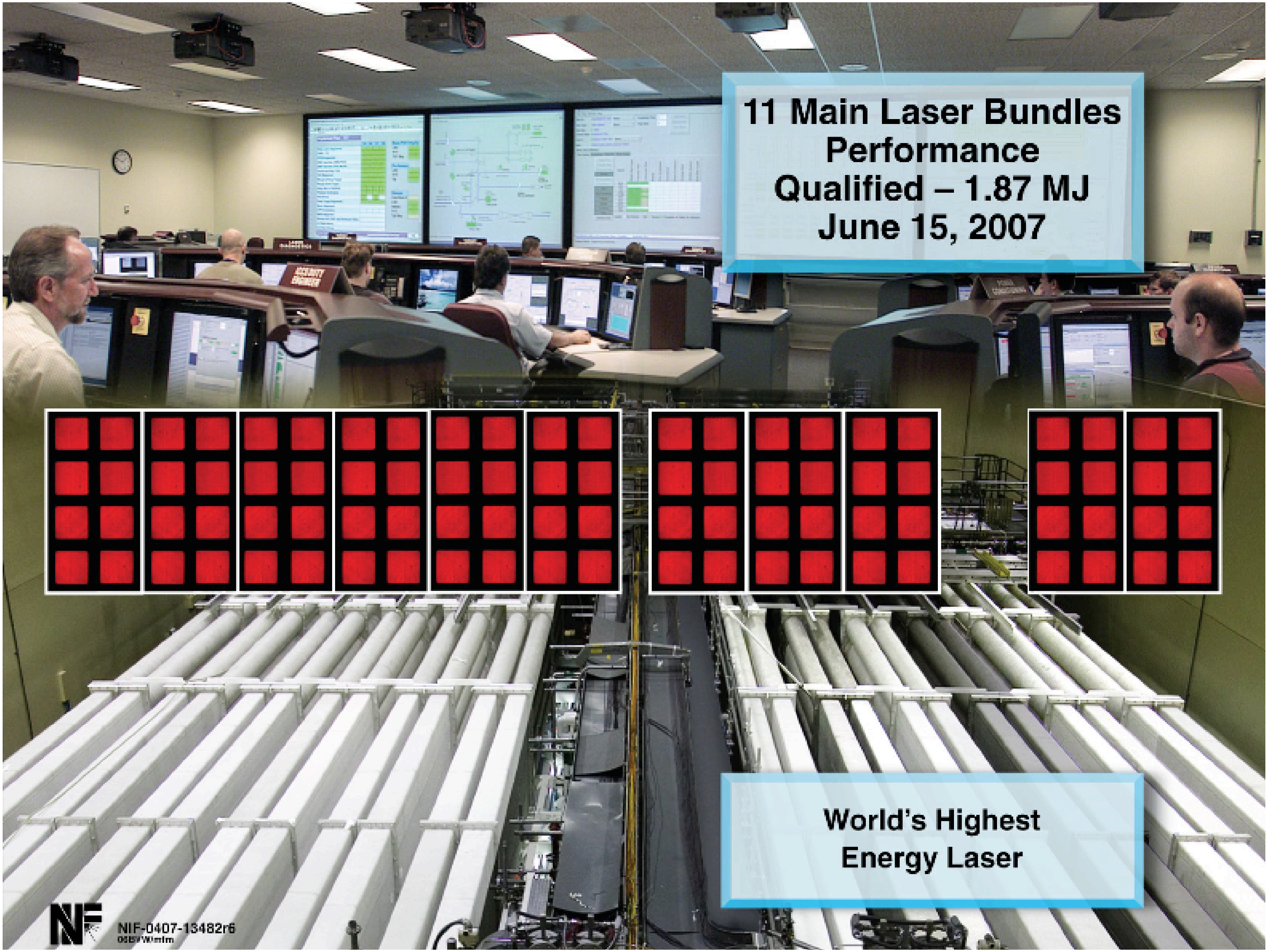
11 Main Laser Bundles
Performance
Qualified – 1.87 MJ
June 15, 2007
World's Highest
Energy Laser
NIF-0407-13482r6

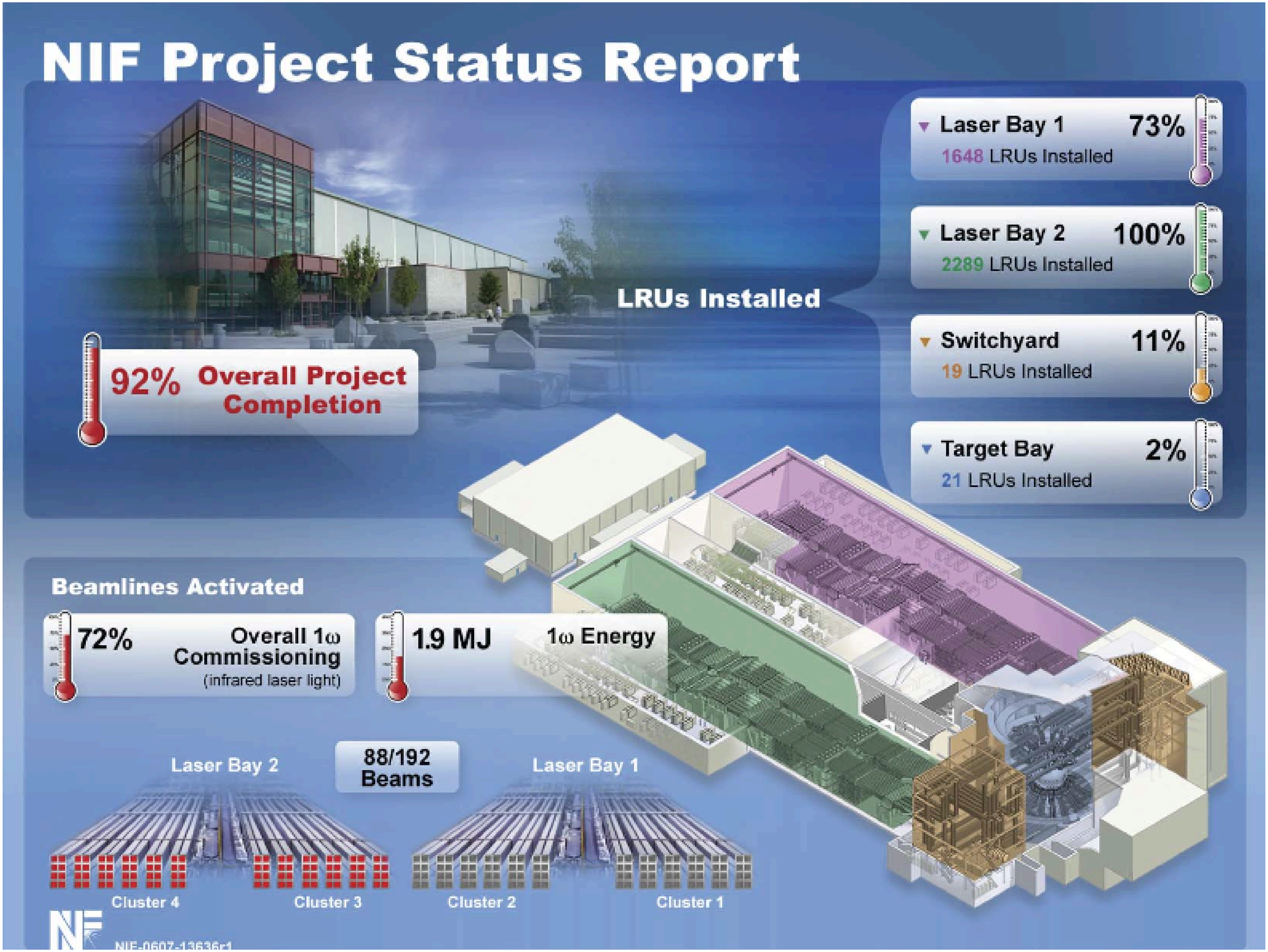

NIF Project Status Report
Laser Bay 1 73%
1648 LRUs Installed
Laser Bay 2 100%
2289 LRUs Installed
LRUs Installed
Switchyard 11%
19 LRUs Installed
Target Bay 2%
21 LRUs Installed
92% Overall Project Completion
Beamlines Activated
72% Overall 1ω Commissioning
(infrared laser light)
1.9 MJ 1ω Energy
Laser Bay 2
88/192 Beams
Laser Bay 1
Cluster 4
Cluster 3
Cluster 2
Cluster 1
NIF-0607-13636r1

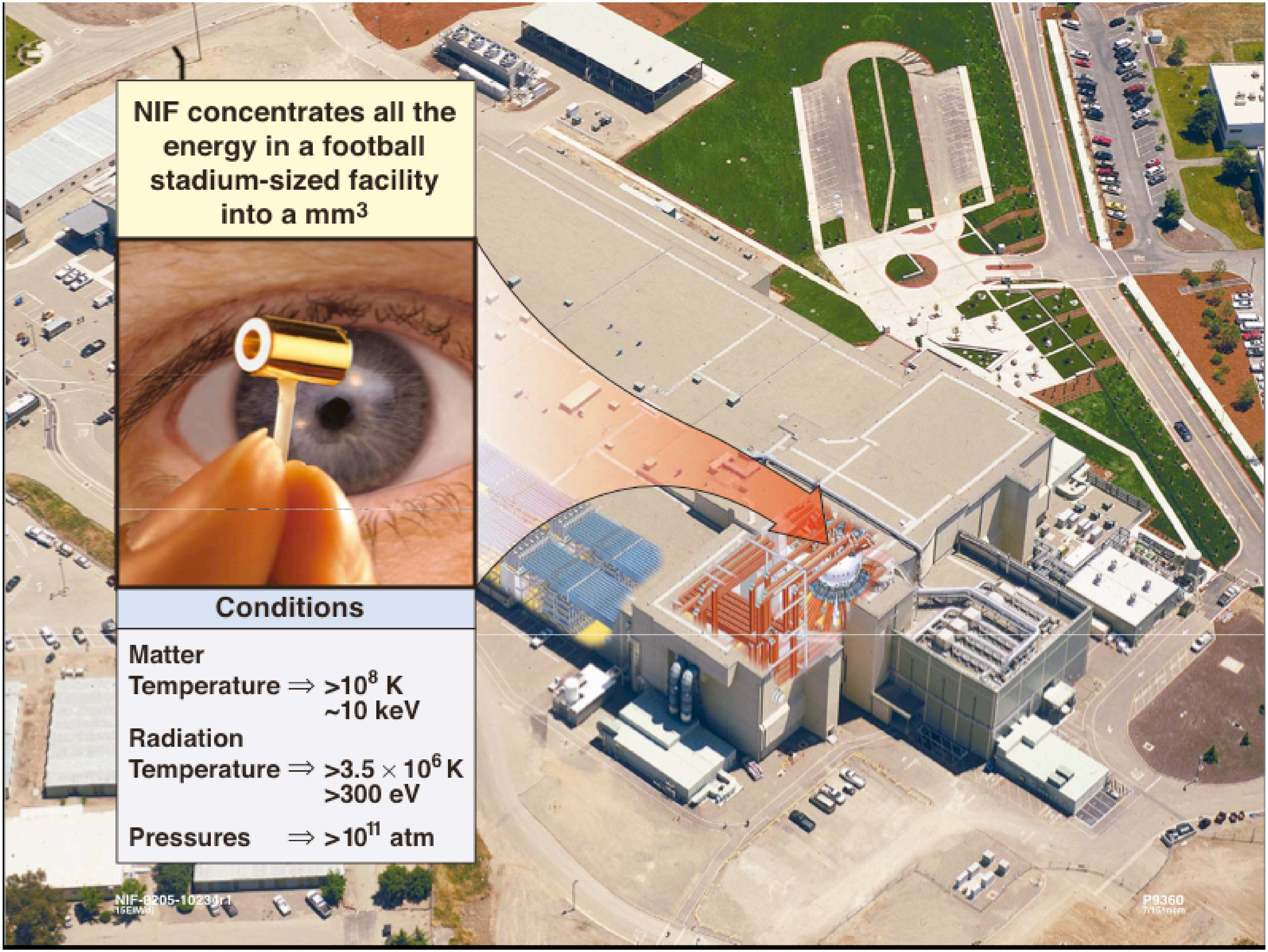
NIF concentrates all the energy in a football stadium-sized facility into a mm³
Conditions
Matter
Temperature ⇒ >10⁸ K ~10 keV
Radiation
Temperature ⇒ >3.5 × 10⁶ K >300 eV
Pressures ⇒ >10¹¹ atm
P9360

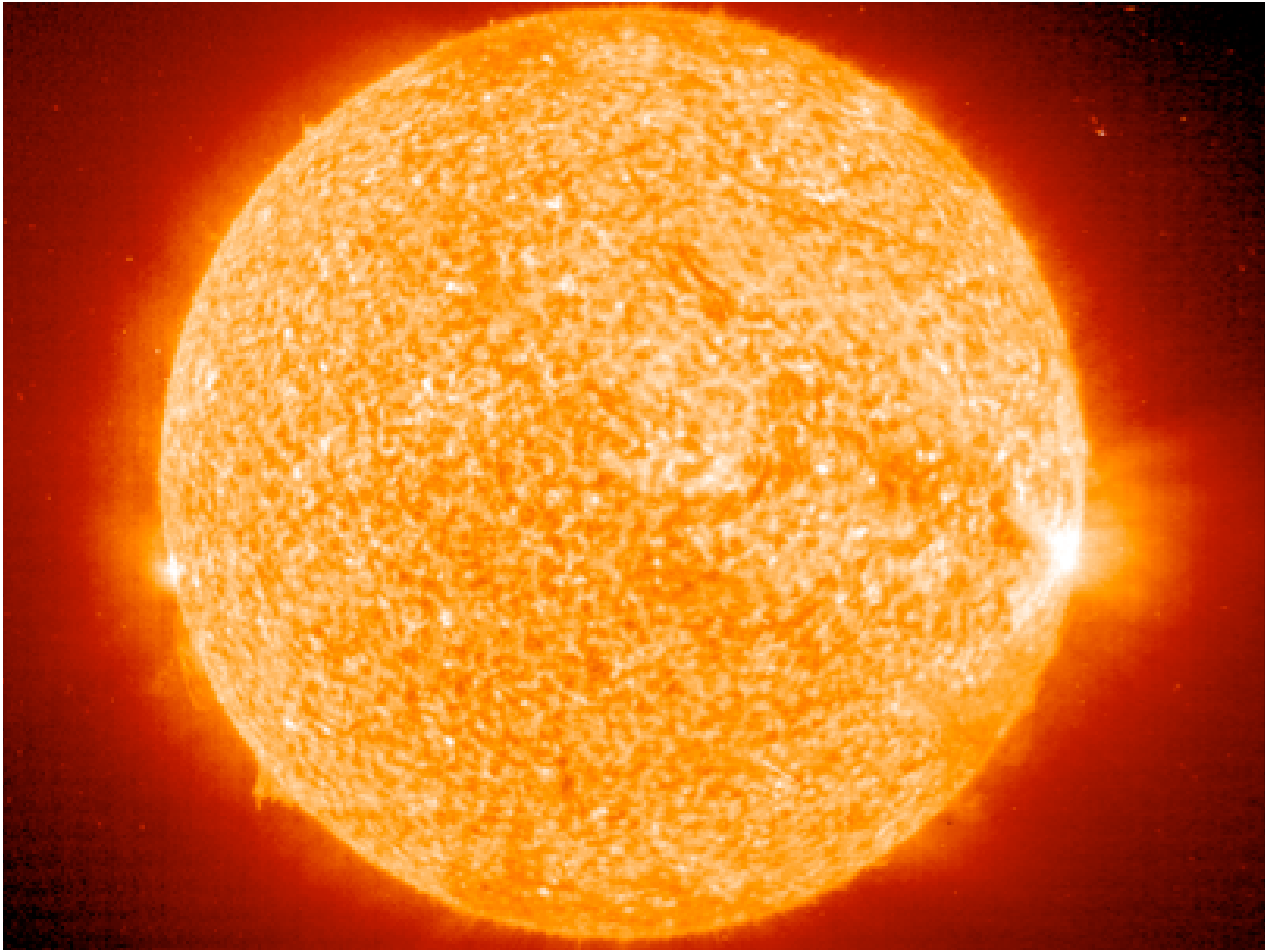

NIF will produce new states of matter that can be directly measured with x-ray scattering

NIF will produce conditions found in stellar interiors (1000 times solid density)

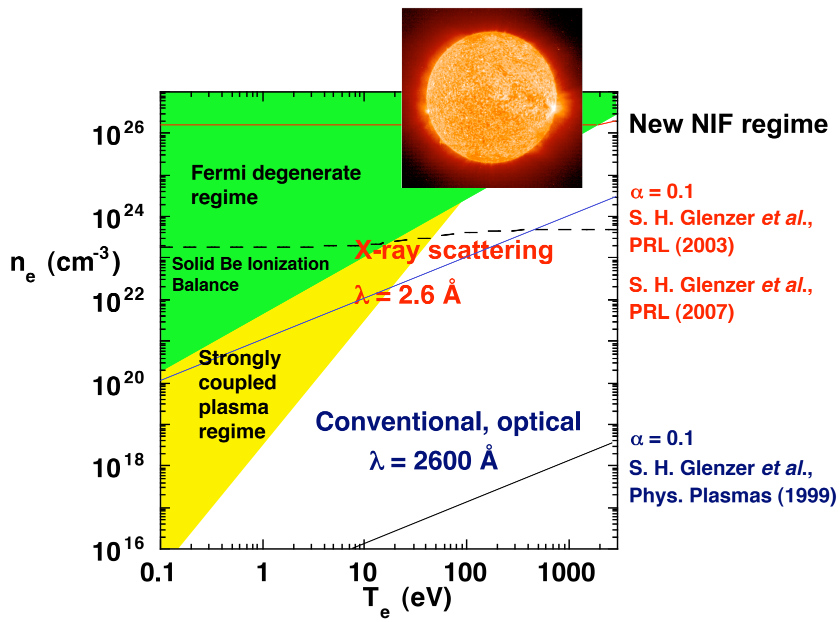

Penetrating x rays are being applied to study the physical properties of dense matter

The National Ignition Facility

Wilhelm Röntgen, first Novel prize in physics, 1901

Röntgen started to take the first radiographs of his wife's hand

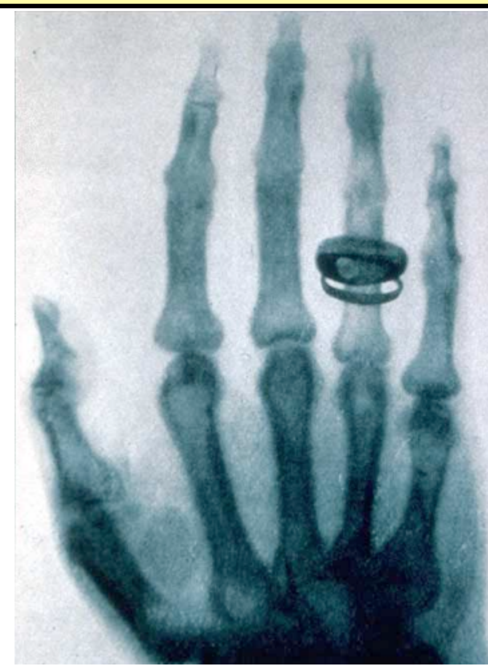

- **Time-resolved X-ray backlighting/ imaging will provide velocity [engineering and laser science problem]**
- **X-ray scattering will determine the physics of dense matter: structure and properties**

NIF will produce new states of matter that can be directly measured with x-ray scattering

The National Ignition Facility

NIF will produce conditions found in stellar interiors (1000 times solid density)

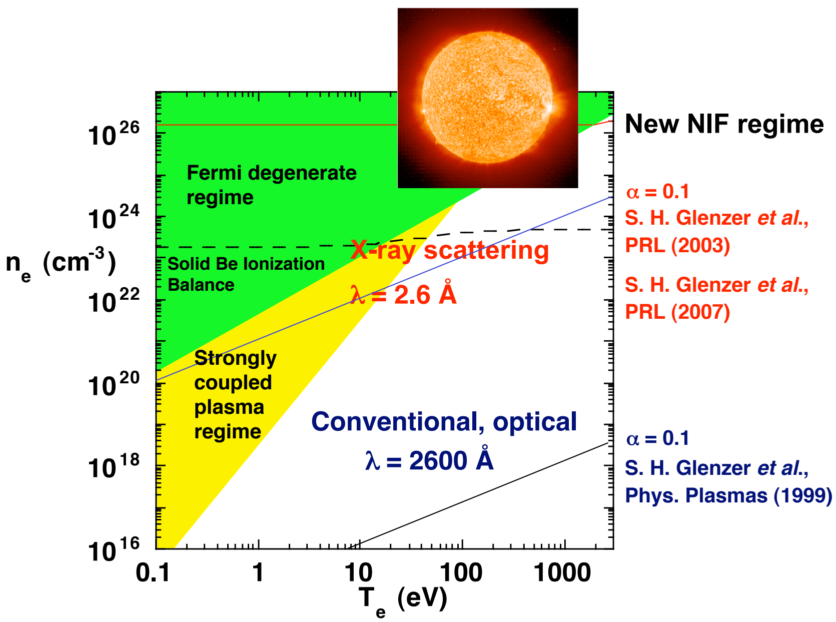

Radiation-hydrodynamic simulations of NIF implosions

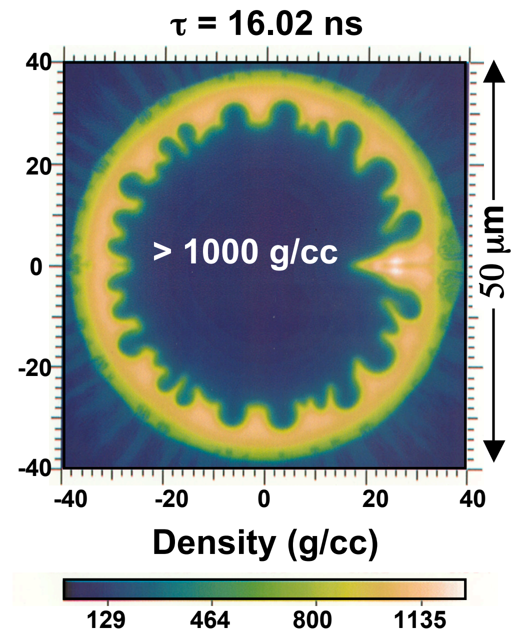

- X-ray scattering provides temperature and density
- Need intense high-energy radiation to penetrate through the capsule and to avoid bremsstrahlung emission
- Determine compression and adiabat of dense plasmas on NIF

From optical ‘Thomson scattering’ to x-ray ‘Compton’ Scattering

The National Ignition Facility

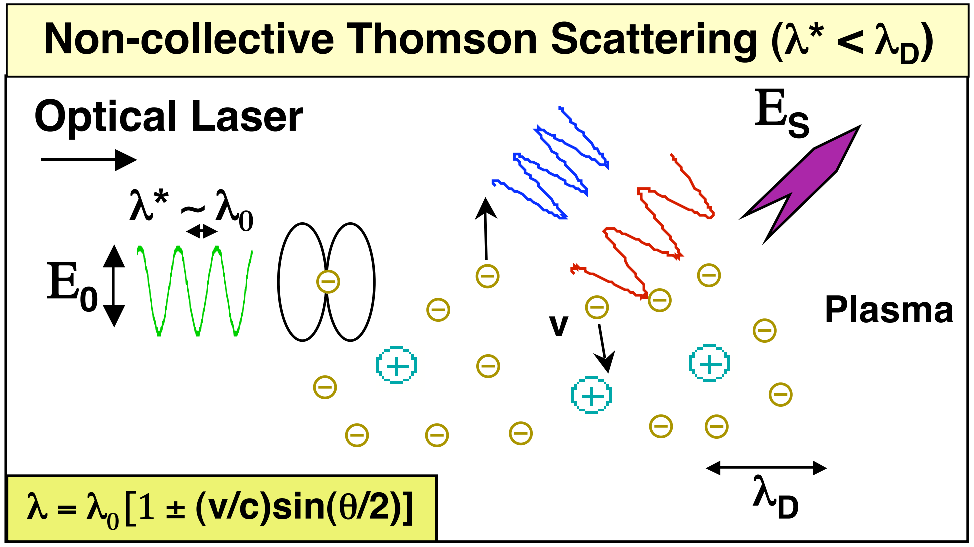

Scattering on free electrons

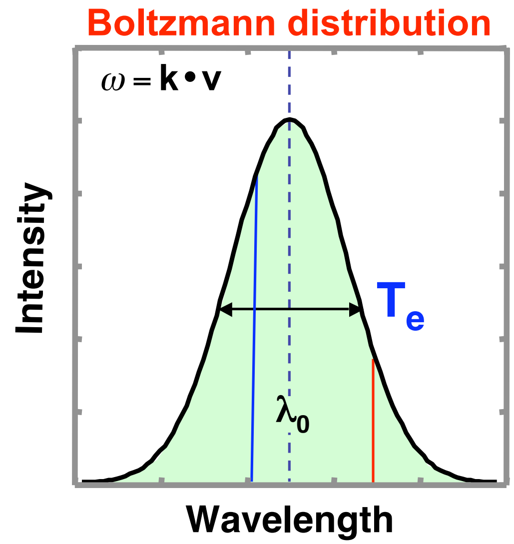

From optical ‘Thomson scattering’ to x-ray ‘Compton’ Scattering

The National Ignition Facility

Non-collective Thomson Scattering ($\lambda^* < \lambda_D$)

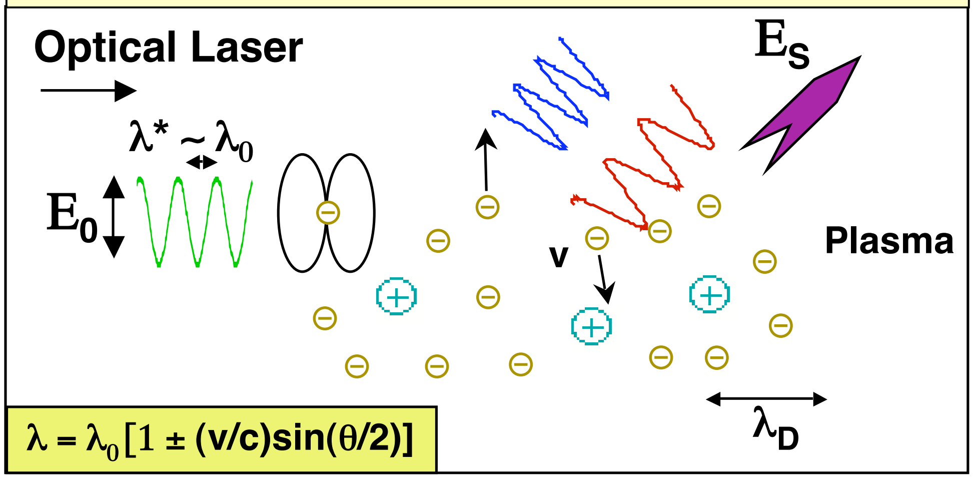

$\lambda = \lambda_0[1 \pm (v/c)\sin(\theta/2)]$

Scattering on free electrons

Boltzmann distribution

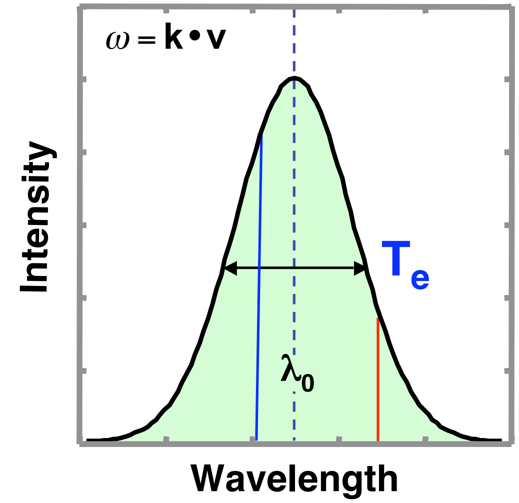

X-ray ‘Compton’ scattering

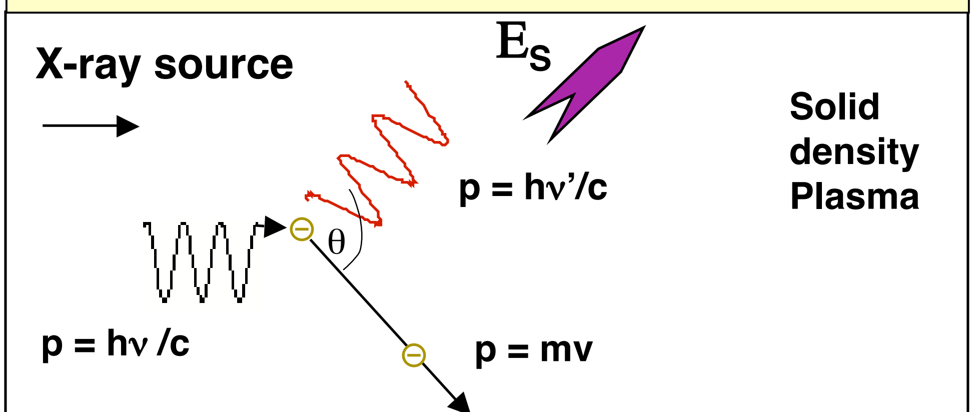

$\lambda = \lambda_0[1 + 2(h\nu/mc^2)\sin^2(\theta/2) \pm (v/c)\sin\theta/2]$

Scattering on free and weakly bound electrons

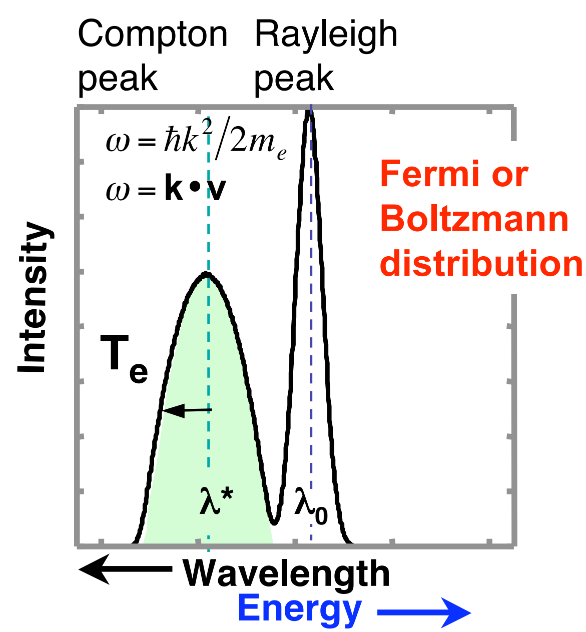

Example of Doppler and Compton shift, and dependence of shape on plasma conditions

The National Ignition Facility

Solid density plasma with:
$T_e = T_i = 12$ eV; $n_e = 3 \times 10^{23}$ cm^{-3}

$$\mathbf{k}_0 = \frac{2\pi}{\lambda_0}$$

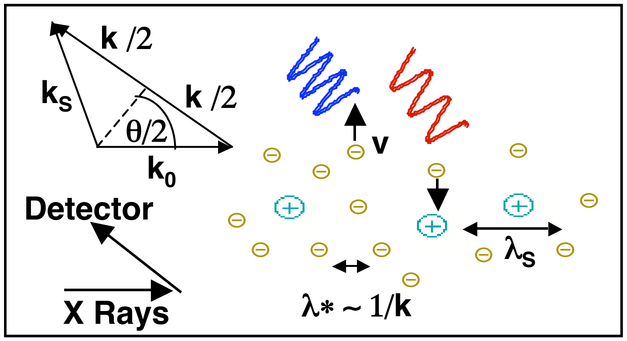

$$\mathbf{k} = 2\mathbf{k_0} \sin\theta/2$$

$$\theta = 110°; \quad E_0 = 4.75 \text{ keV} \rightarrow 2.6\text{Å} \quad [\textbf{Ti He-}\alpha]$$

$$\text{k} = 4 \times 10^{-10}\text{m}^{-1} \rightarrow \lambda^* = 1.6\text{Å}$$

Compare with screening length [Debye length]:

$$\lambda_S \approx \lambda_D = 0.5\text{Å}$$

$$\alpha = \frac{1}{k\lambda_S} = \frac{\lambda^*}{2\pi\lambda_S} \approx 0.5$$

Individual e$^-$ motion is observed

$$\omega = \Delta\omega = \frac{2\pi c}{\lambda_0} - \frac{2\pi c}{\lambda} = \mathbf{k} \bullet \mathbf{v}$$

Doppler effect

Example of Doppler and Compton shift, and dependence of shape on plasma conditions

The National Ignition Facility

Solid density plasma with:
$T_e = T_i = 12$ eV; $n_e = 3 \times 10^{23}$ cm^{-3}

$$\mathbf{k}_0 = \frac{2\pi}{\lambda_0}$$

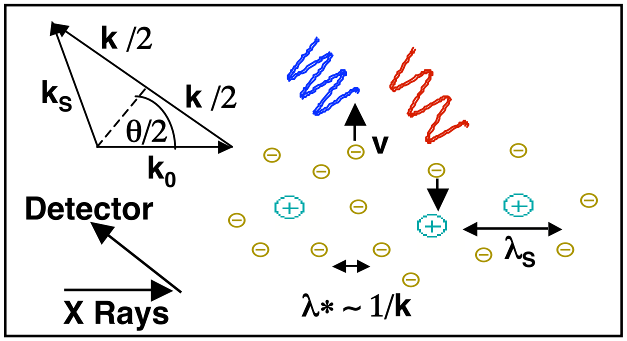

$$\mathbf{k} = 2\mathbf{k_0}\sin\theta/2$$

$$\theta = 110°; \quad E_0 = 4.75 \text{ keV} \rightarrow 2.6\text{Å} \quad [\textbf{Ti He-}\alpha]$$

$$\text{k} = 4 \times 10^{-10}\text{m}^{-1} \rightarrow \lambda^* = 1.6\text{Å}$$

Compare with screening length [Debye length]:

$$\lambda_S \approx \lambda_D = 0.5\text{Å}$$

$$\alpha = \frac{1}{k\lambda_S} = \frac{\lambda^*}{2\pi\lambda_S} \approx 0.5$$

Individual e$^-$ motion is observed

$$\omega = \Delta\omega = \frac{2\pi c}{\lambda_0} - \frac{2\pi c}{\lambda} = \mathbf{k \bullet v}$$

Doppler effect

3-D velocity space

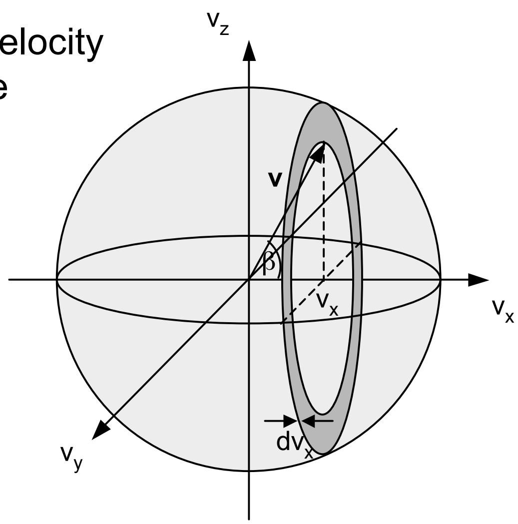

$$f(v_x)dv_x = \int_{v_x}^{v=\infty} \underbrace{n(v)}_{\text{Occupancy}} \underbrace{2\pi\sqrt{v^2 - v_x^2}}_{\text{Circumference}} \underbrace{\frac{dv}{\sin\beta}}_{\text{Width}} \underbrace{dv_x}_{\text{Thickness}}$$

$$use: \quad v_x = v\cos\beta; v_F = \sqrt{2\varepsilon_F / m_e}$$

$$f\left(\frac{v_x}{v_F}\right) = \int_0^{2\pi} \frac{(v_x/v_F\cos\beta)^2\tan\beta d\beta}{\exp\left(\left((v_x/v_F\cos\beta)^2 - 1 + (\pi^2/12)(T_e/\varepsilon_F)^2\right)\Big/(T_e/\varepsilon_F)\right)+1}$$

$$\varepsilon_F = \frac{\hbar^2}{2m_e}(3\pi^2 n_e)^{2/3} = 17\text{eV}; \qquad f(E) = \frac{1}{\exp((E-\varepsilon_F)/T_e)+1}$$

Example of Doppler and Compton shift, and dependence of shape on plasma conditions

The National Ignition Facility

Solid density plasma with:
$T_e = T_i = 12$ eV; $n_e = 3 \times 10^{23}$ cm^{-3}

$$\mathbf{k}_0 = \frac{2\pi}{\lambda_0}$$

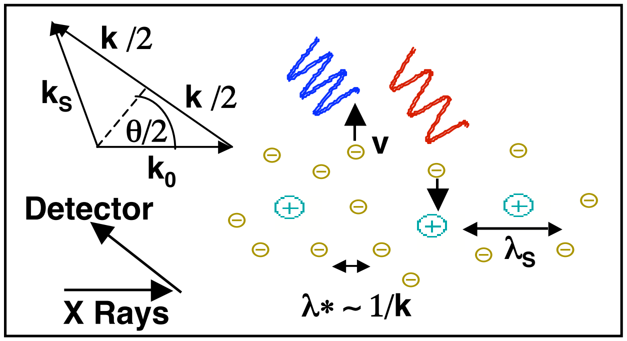

$$\mathbf{k} = 2\mathbf{k_0} \sin\theta/2$$

$$\theta = 110°; \quad E_0 = 4.75 \text{ keV} \rightarrow 2.6\text{Å} \quad [\textbf{Ti He-}\alpha]$$

$$\text{k} = 4 \times 10^{-10}\text{m}^{-1} \rightarrow \lambda^* = 1.6\text{Å}$$

Compare with screening length [Debye length]:

$$\lambda_S \approx \lambda_D = 0.5\text{Å}$$

$$\alpha = \frac{1}{k\lambda_S} = \frac{\lambda^*}{2\pi\lambda_S} \approx 0.5$$

Individual e$^-$ motion is observed

$$E_C = \frac{\hbar^2 k^2}{2m_e} = 58\text{eV}$$

$$\omega = \Delta\omega = \frac{2\pi c}{\lambda_0} - \frac{2\pi c}{\lambda} = \mathbf{k \bullet v}$$

Doppler effect

Occupancy Circumference Width Thickness

$$f(v_x)dv_x = \int_{v_x}^{v=\infty} n(v) 2\pi\sqrt{v^2 - v_x^2}\, \frac{dv}{\sin\beta}\, dv_x$$

$$use: \quad v_x = v\cos\beta;\ v_F = \sqrt{2\varepsilon_F/m_e}$$

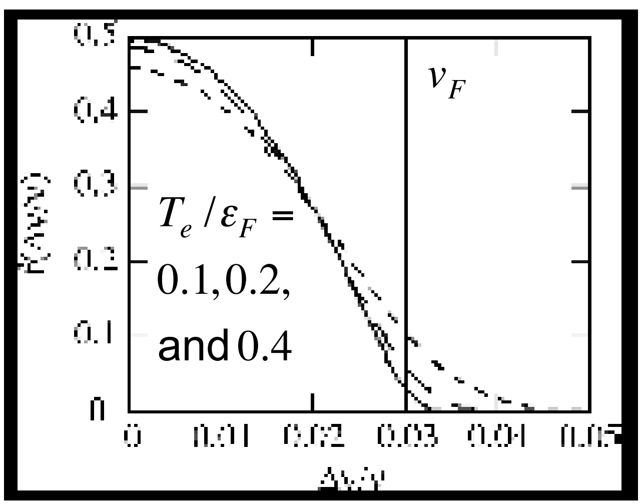

$$f\left(\frac{v_x}{v_F}\right) = \int_0^{2\pi} \frac{\left(v_x/v_F\cos\beta\right)^2 \tan\beta\, d\beta}{\exp\left(\left(\left(v_x/v_F\cos\beta\right)^2 - 1 + \left(\pi^2/12\right)\left(T_e/\varepsilon_F\right)^2\right)\Big/\left(T_e/\varepsilon_F\right)\right) + 1}$$

$$\varepsilon_F = \frac{\hbar^2}{2m_e}\left(3\pi^2 n_e\right)^{2/3} = 17\text{eV}; \qquad f(E) = \frac{1}{\exp\left((E - \varepsilon_F)/T_e\right) + 1}$$

From optical ‘Thomson scattering’ to x-ray ‘Compton’ Scattering

The National Ignition Facility

Non-collective Thomson Scattering ($\lambda^* < \lambda_D$)

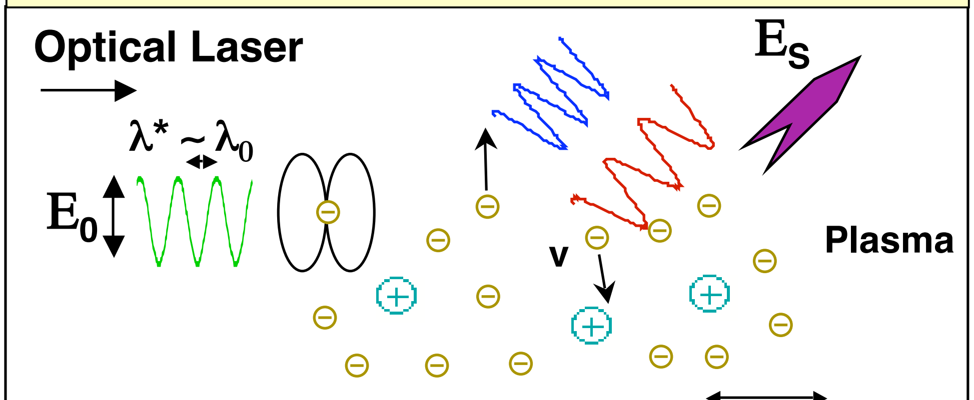

$\lambda = \lambda_0[1 \pm (v/c)\sin(\theta/2)]$

Scattering on free electrons

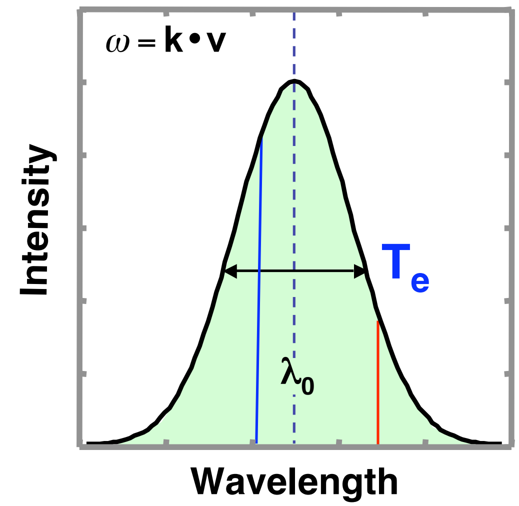

X-ray ‘Compton’ scattering

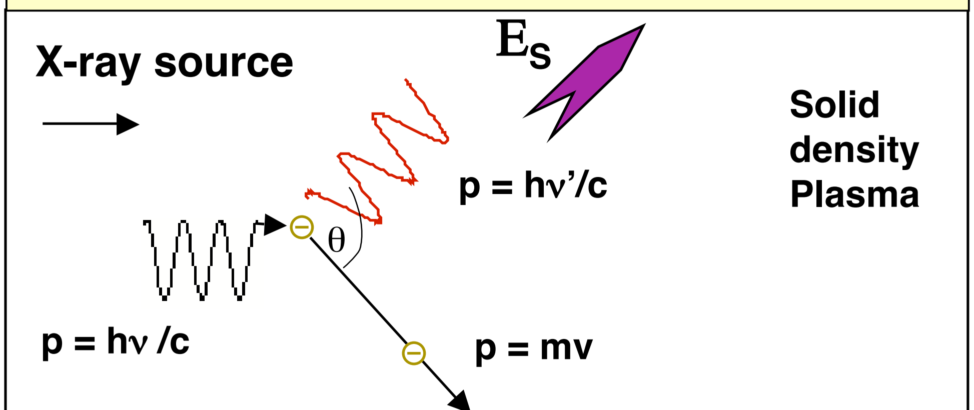

$\lambda = \lambda_0[1 + 2(h\nu/mc^2)\sin^2(\theta/2) \pm (v/c)\sin\theta/2]$

Scattering on free and weakly bound electrons

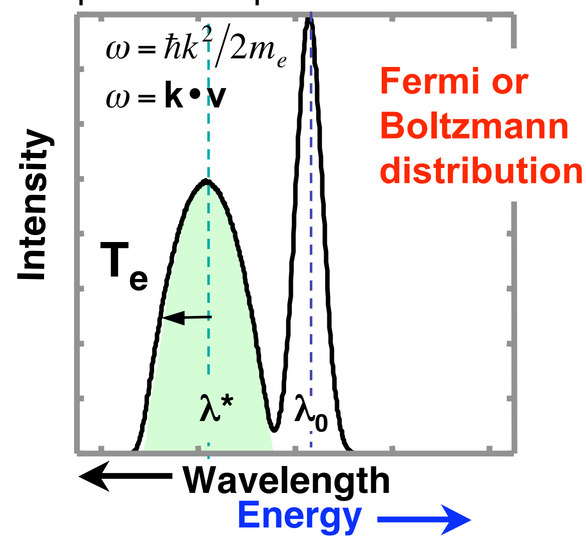

X-ray scattering divided between elastic (Rayleigh) and inelastic (free plus weakly bound) components

The National Ignition Facility

Elastic

Tightly bound e^-
I.P. > $(h\nu/m_ec^2)h\nu$

Tightly bound electrons give Rayleigh peak and correction to the Compton shift

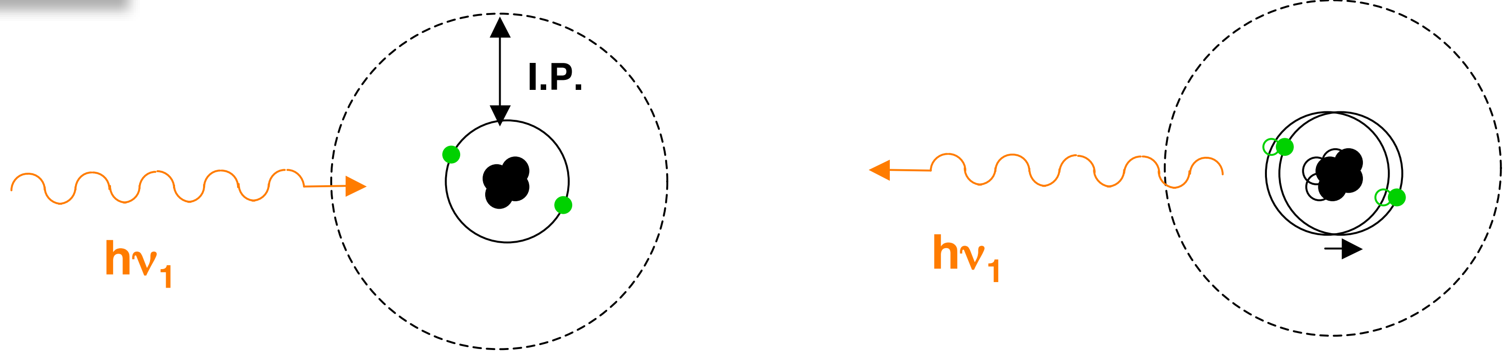

Inelastic

Weakly bound e^-
I.P. < $(h\nu/m_ec^2)h\nu$

$\Delta E_e = (h\nu/m_ec^2)h\nu$

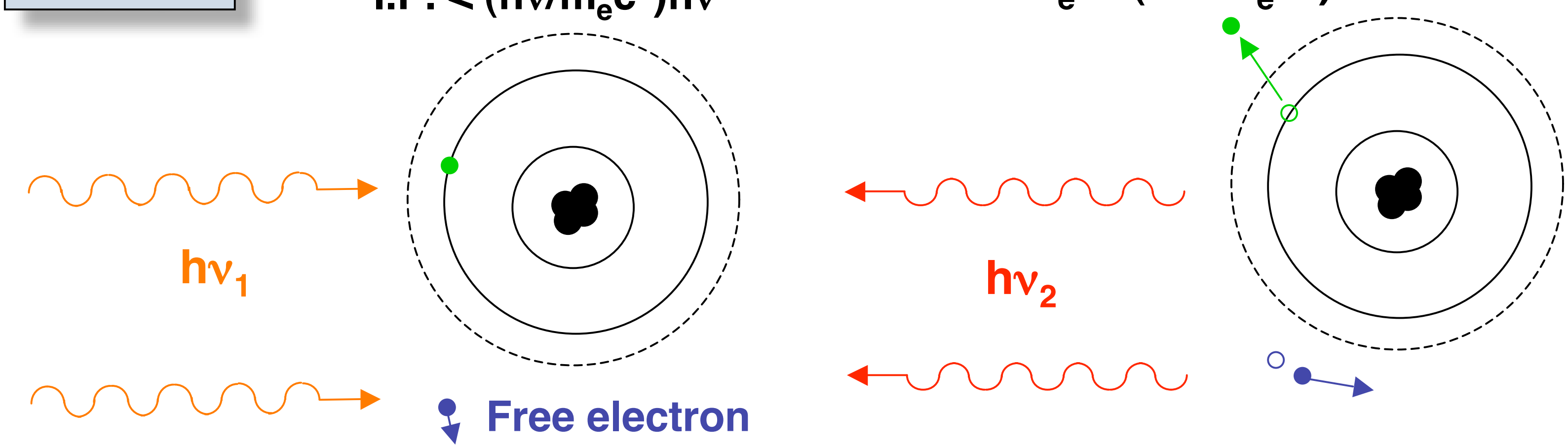

O. L. Landen et al., JQSRT 71, 465 (2001):

$h\nu_2 = h\nu_1 - (h\nu/m_ec^2)h\nu(1-\cos\theta)$ (Compton) $\pm\ 2h\nu(v_e/c)\sin\theta/2$ (Doppler)

Max. θ: ⇒ max. Compton shift
max. Doppler broad.

X-ray Thomson scattering has been shown to accurately characterize dense compressed matter

- Introduction
  - X-ray Thomson scattering from solid density plasmas
- **Proof of principle experiments**
  - **Backscattering experiment**
    - **Compton scattering in dense plasmas**
    - **Accurate temperature diagnostics**
  - **Forward scattering experiment**
    - **First observation of Plasmons in Warm Dense Matter**
    - **Accurate density diagnostic**
    - **Importance of collisions**
- Compressed Matter
  - Compressibility and adiabat
  - Structure Factors
  - Coalescing shocks
- Outlook and Conclusions

X-ray "Thomson' scattering in warm solid density matter was first demonstrated on beryllium at the Omega laser

Experiment

The National Ignition Facility

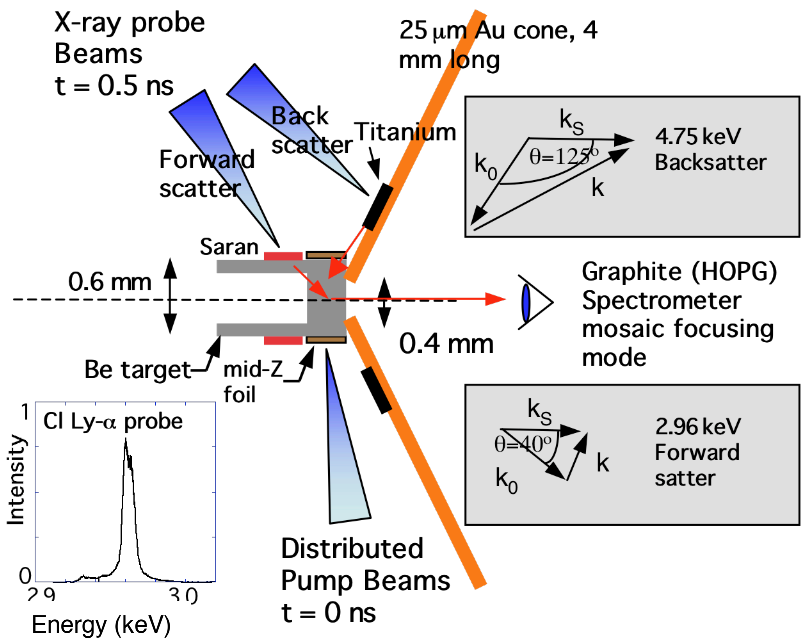

Compton downshifted and Doppler broadened Thomson spectrum observed as expected

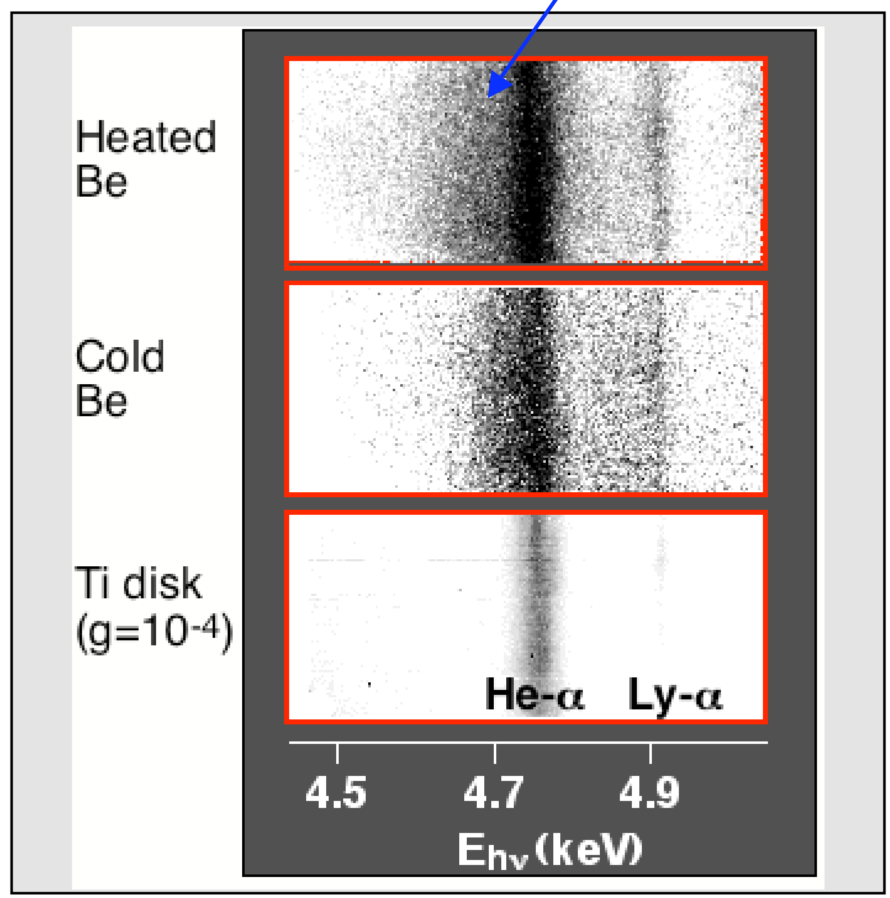

- T_e broadening was predicted in 1928: Chandrasekhar: "scattering will not be influenced by ranges of temperatures available in the laboratory"
  Proc R.S. A 125, 37 (1929)

S. H. Glenzer et al., Phys. Rev. Lett. 90, 175002 (2003).

Experiment

The theoretical form factor for x-ray scattering provides reliable plasma parameter for back scatter experiments

The National Ignition Facility

Probe

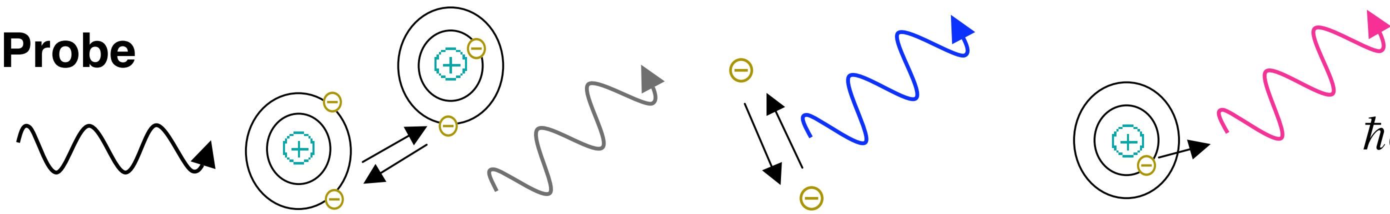

$$\hbar\omega = \hbar\omega_1 - \hbar\omega_0$$

$$S(k,\omega) = \underbrace{\left|f_I(k) + q(k)\right|^2 S_{ii}(k,\omega)}_{\text{Ion feature}} + \underbrace{Z_f S_{ee}^0(k,\omega)}_{\text{Electron feature}} + \underbrace{Z_b \int \tilde{S}_{ce}(k,\omega-\omega')S_s(k,\omega')d\omega'}_{\text{Bound-free}}$$

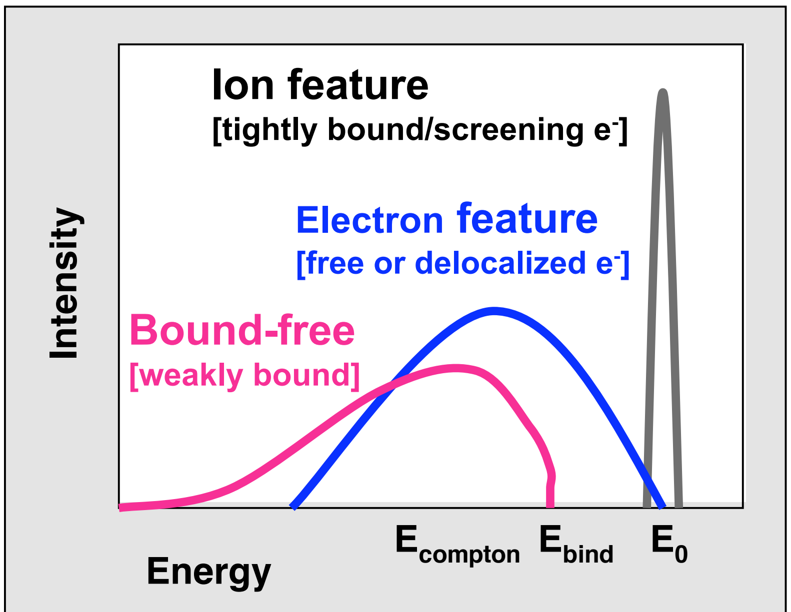

Schematic Scattering spectrum

- Free or delocalized electrons result in the Compton down-shifted line, $Z_f\ S_{ee}\ (k,\omega)$
- Bound-free contribution also results into down-shifted spectrum
- $Z_b\ S_{ce}\ (k,\omega)$
- The momentum of bound e^- causes broadening
- The ion feature describes elastic scattering $S_{ii}(k,\omega)$
- In backscatter: theoretical approximations agree

Chihara, PRE (2000), Gregori et al, PRE (2003)

X-ray scattering provides accurate temperature measurements in solid-density Be plasmas

X-ray scattering spectra provide accurate data on T_e and n_e

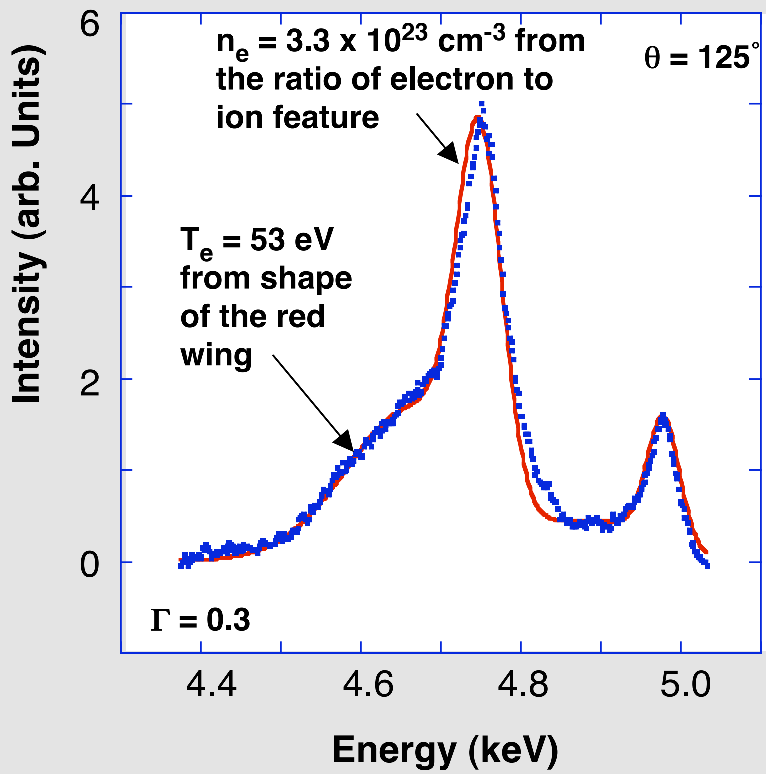

From the theoretical fit to the data:
T_e = 53 eV and Z_{free} = 3.1 corresponding to $n_e = 3.8 \times 10^{23}$ cm^{-3}

Comparison of experimental data with theoretical calculations for various T_e

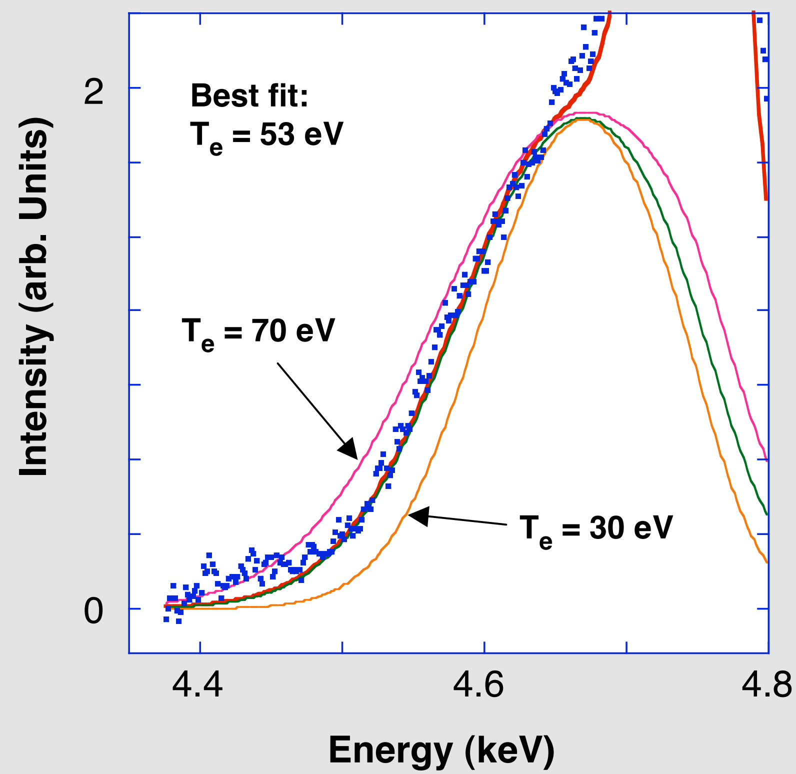

A sensitivity analysis shows that we can measure T_e with an error bar of ~15%

Experiment

The National Ignition Facility

X-ray scattering application: test of ionization balance models in dense plasmas

Ionization balance of Carbon compares well to calculations [FLY, Comptra]

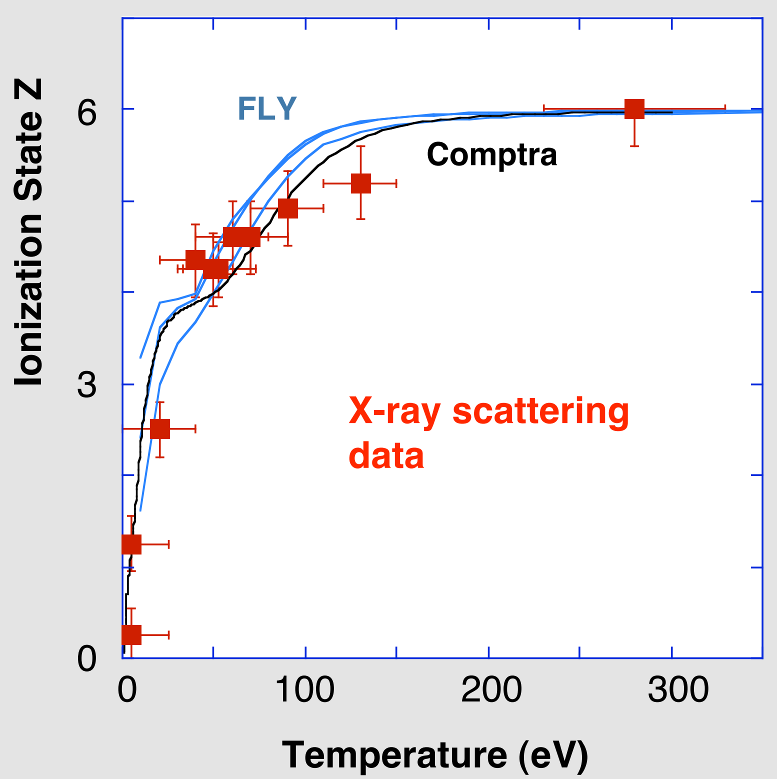

X-ray scattering has been successfully applied in different targets varying in density from $10^{21} < n_e < 10^{23}$ cm^{-3}

Gregori et al, JQSRT (2006)

Electron density can be inferred from the Ionization balance of Beryllium

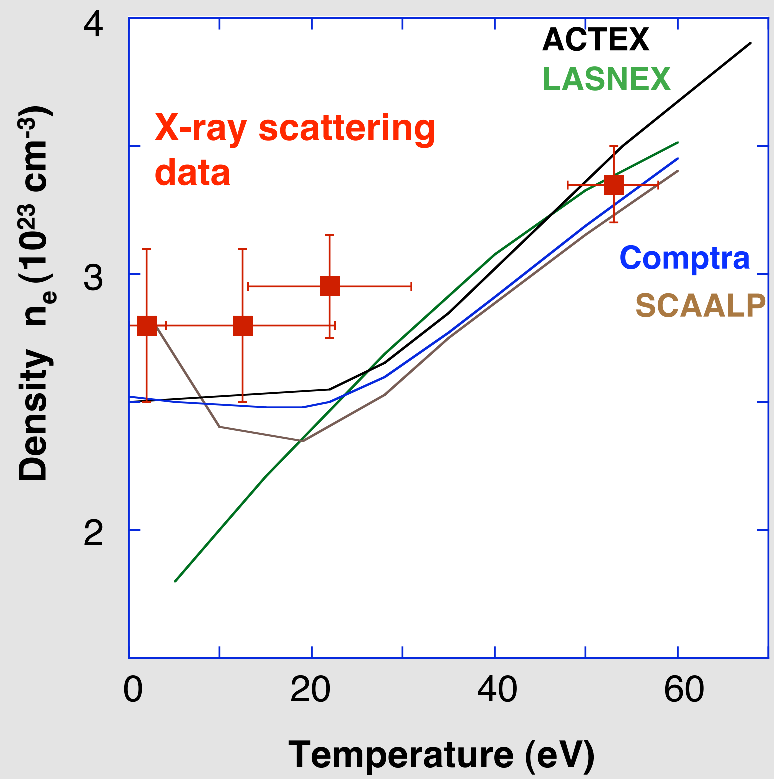

In isochorically heated matter we have: $n_e = 6 \times 10^{23}$ Z/A ρ cm-3 and with $\rho = 1.85$ for Be and Z = 2.5: $n_e = 3 \times 10^{23}$ cm^{-3}

Glenzer et al, PoP (2003)

Experiment

The National Ignition Facility

X-ray scattering application: test of ionization balance models in dense plasmas

Ionization balance of Carbon compares well to calculations [FLY, Comptra]

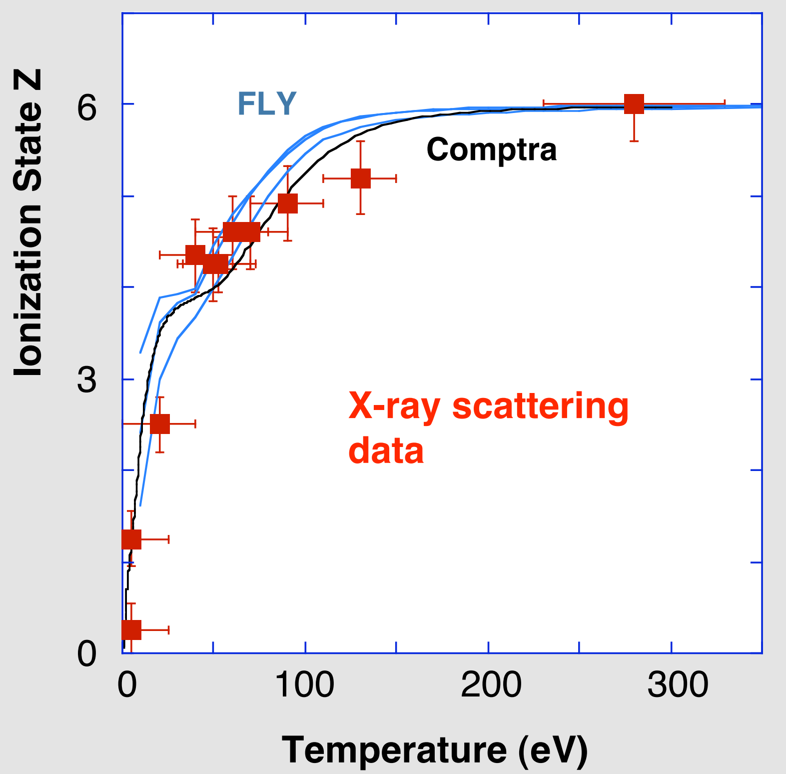

X-ray scattering has been successfully applied in different targets varying in density from $10^{21} < n_e < 10^{23}$ cm^{-3}

Gregori et al, JQSRT (2006)

Electron density can be inferred from the Ionization balance of Beryllium

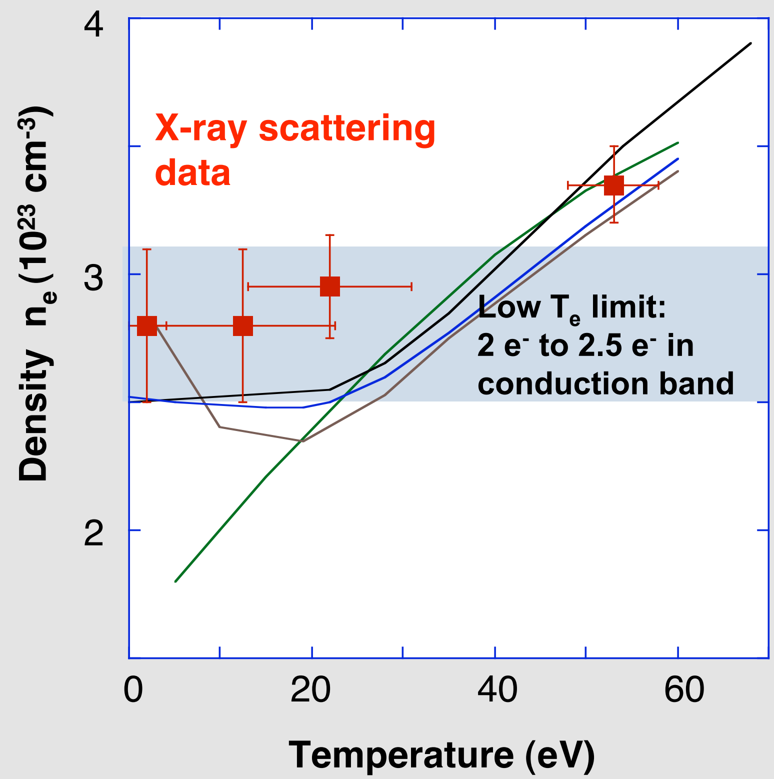

In isochorically heated matter we have: $n_e = 6 \times 10^{23}$ Z/A ρ cm-3 and with $\rho = 1.85$ for Be and Z = 2.5: $n_e = 3 \times 10^{23}$ cm^{-3}

Glenzer et al, PoP (2003)

Experiment

Back- and forward scatter have been demonstrated on Omega accurately characterizing solid-density plasmas

Compton (back-) scatter measures T_e from broadening

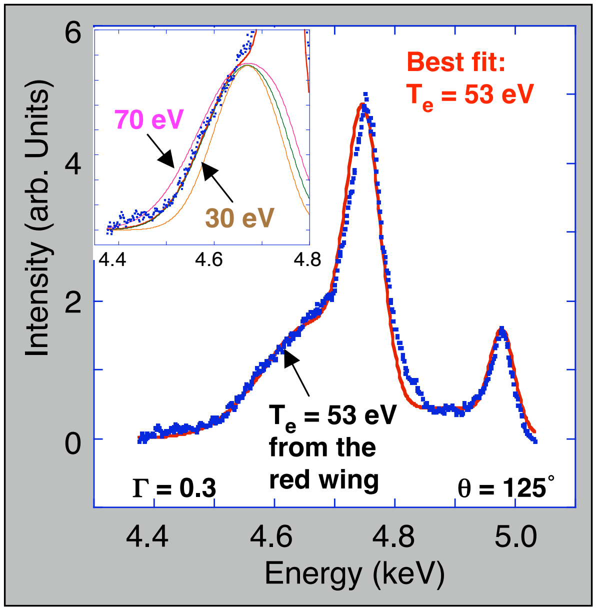

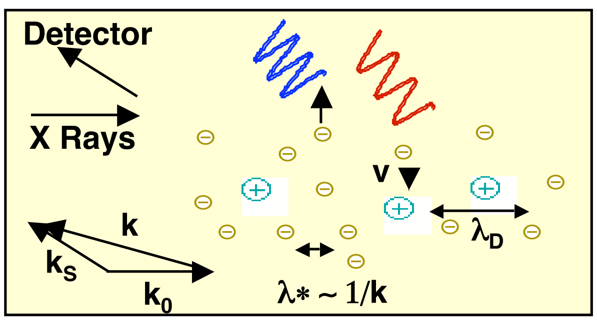

Forward scatter on Plasmons measures n_e from shift

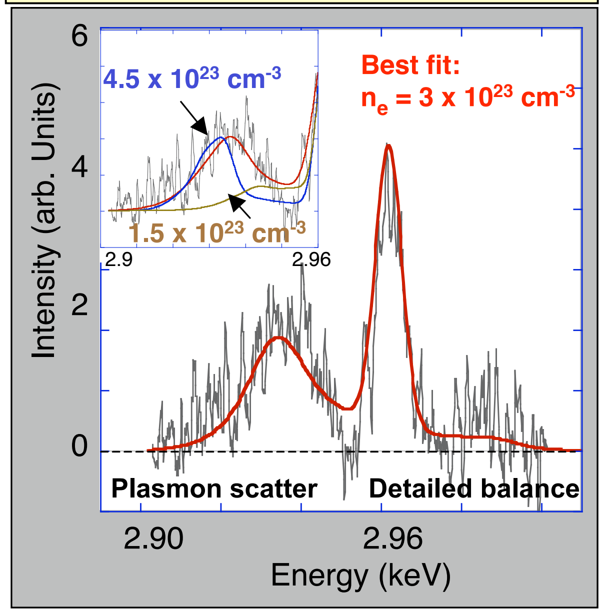

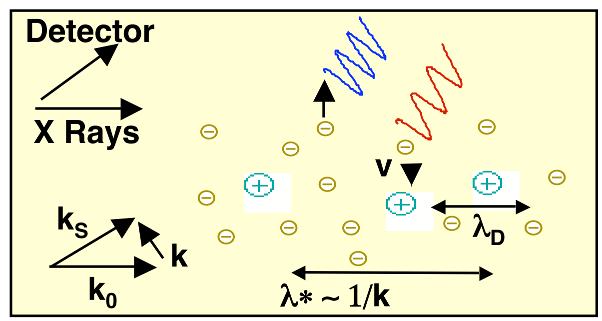

$$\lambda^* > \lambda_S \quad or \quad \alpha = \frac{\lambda^*}{\lambda_S} = \frac{k^{-1}}{\lambda_S} = \frac{\lambda_0}{4\pi\ \lambda_S \sin(\theta/2)} > 1$$

The plasmon frequency provides a robust measure of the density

Density from Plasmon frequency agrees with Z = 2.5 from backscattering

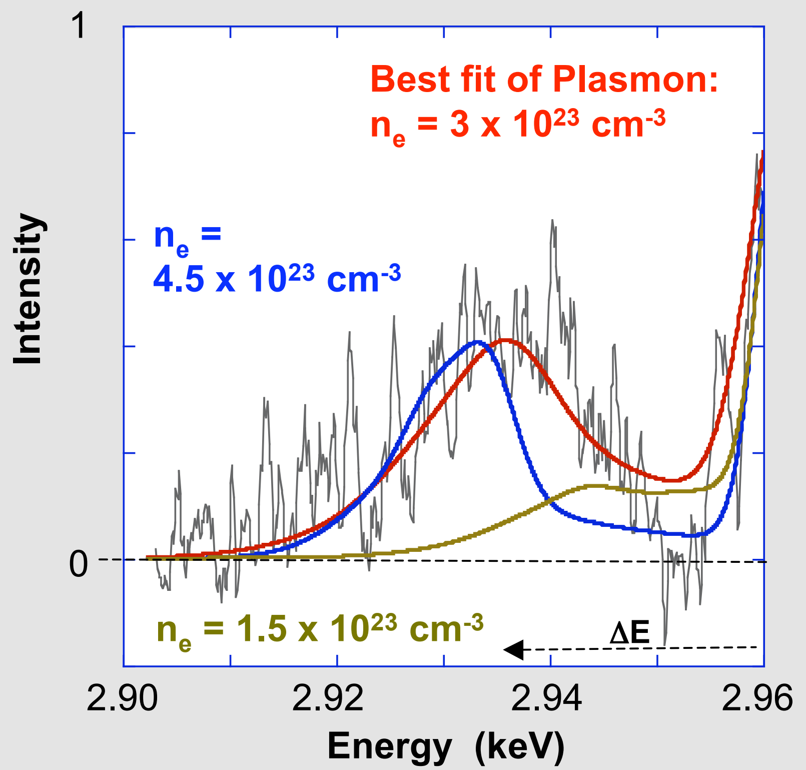

Sensitivity analysis shows error bar in electron density of ~25%
[Reducing noise will improve this value]

The plasmon frequency provides a robust measure of the density

Experiment

The National Ignition Facility

Density from Plasmon frequency agrees with Z = 2.5 from backscattering

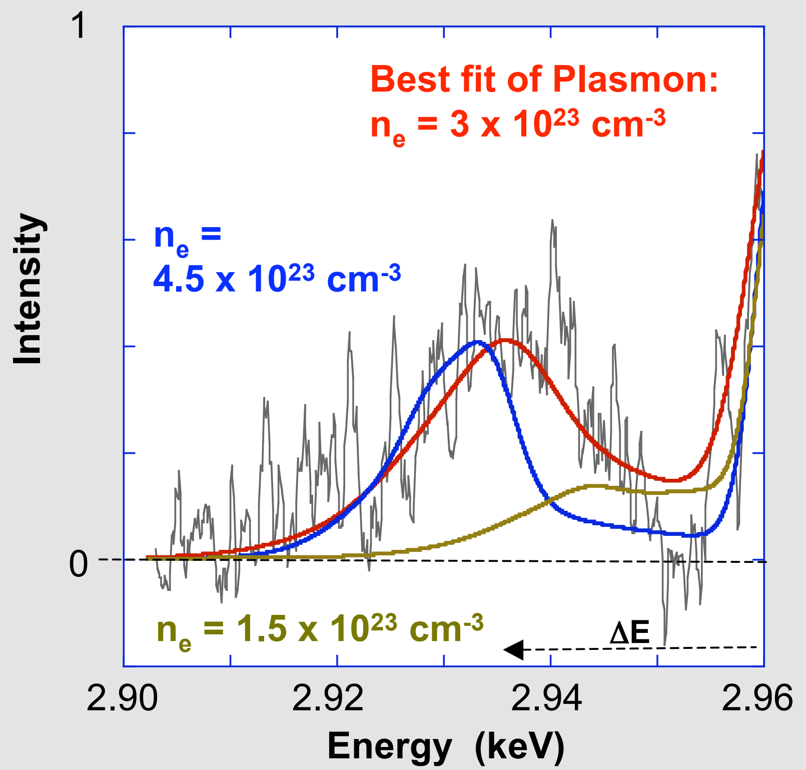

Sensitivity analysis shows error bar in electron density of ~25%
[Reducing noise will improve this value]

Plasmon dispersion relation indicates accurate density measurement

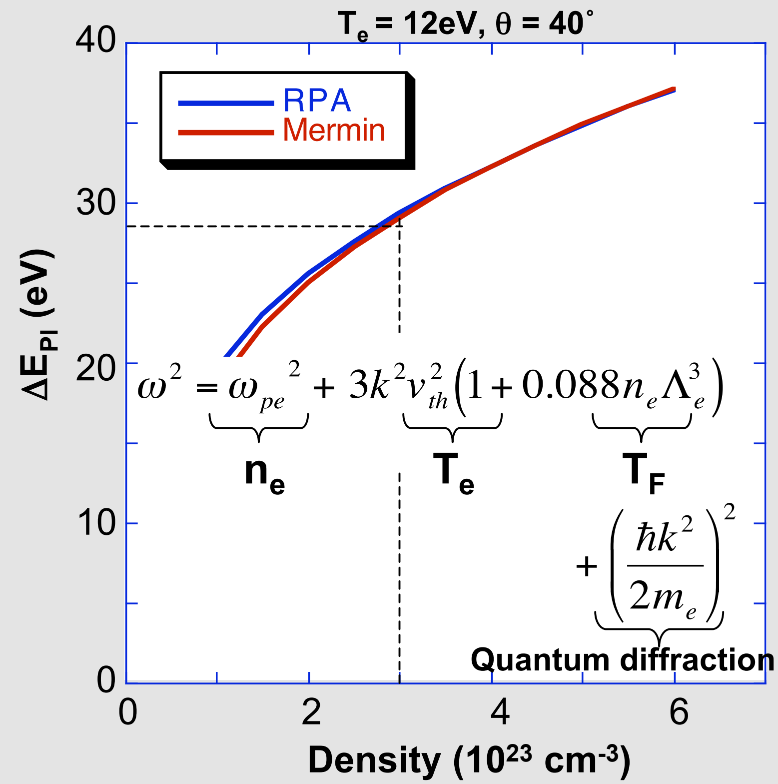

- Leading term is density sensitive (ω_{pe})
- Diffraction is determined by θ and E_0
- Thermal correction (T_e) is of order E_C

Plasmon spectra have been shown to be sensitive to collisions, a fact that can be used to measure conductivity

The National Ignition Facility

Plasmon width is determined by Landau and collisional damping

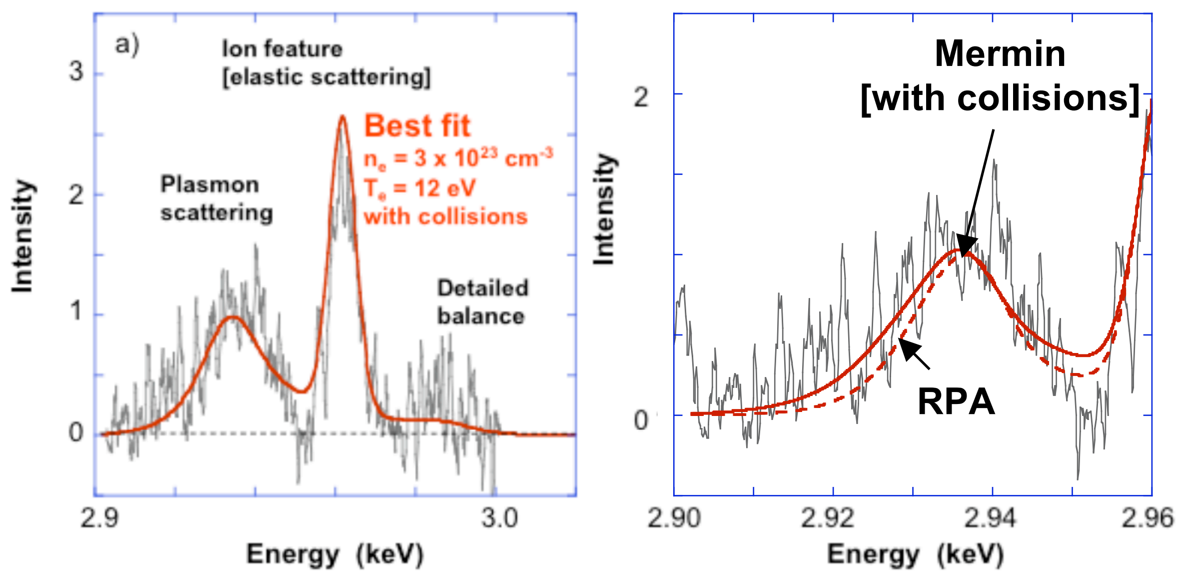

Dashed curved is collision-less theory: Random Phase Approximation

Solid curves use Mermin theory with collisions, ν_{ei}, in Born approximation

- Here, collisions provide a correction to the width [important to obtain fit with proper $T_e$values
- To accurately determine n_{ei} and conductivity we will implement improvements access the collision dominated regime
  - FEL experiment [A. Höll et al, HEDP 3 (2007)]
  - New experiments with lower x-ray energy on Omega

S. H. Glenzer et al., Phys. Rev. Lett. 98, 065002 (2007).

Forward scattering provides n_e and T_e data consistent with previous backscatter measurements and simulations

Radiation-hydrodynamics simulations indicate homogeneous solid density plasma by isochoric heating

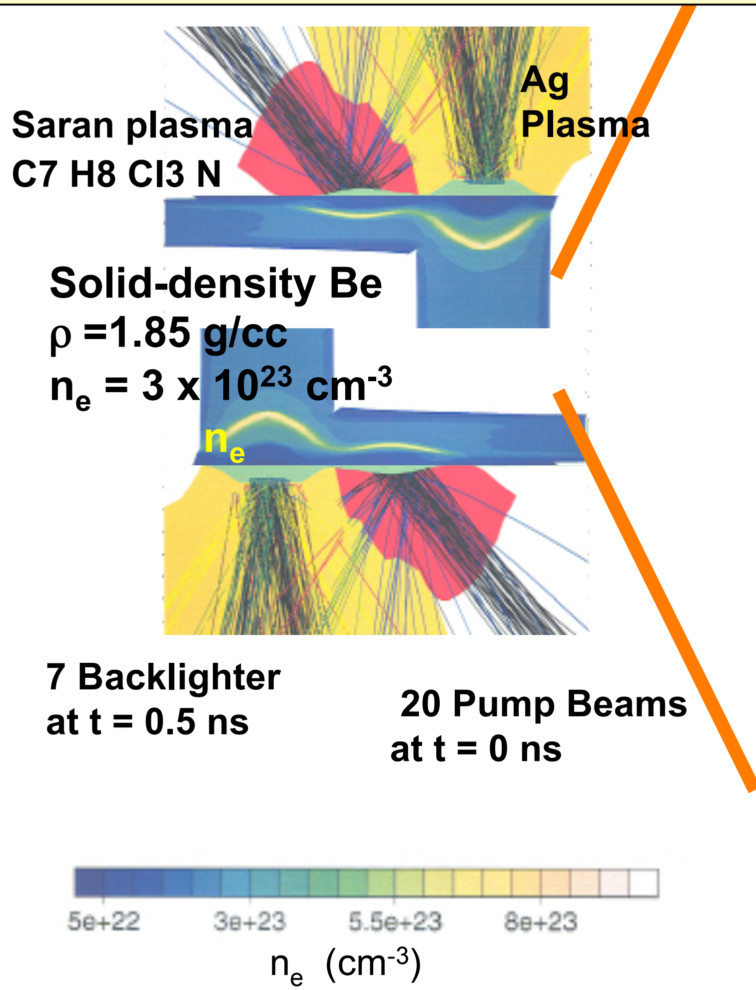

Comparison of experimental data and simulations

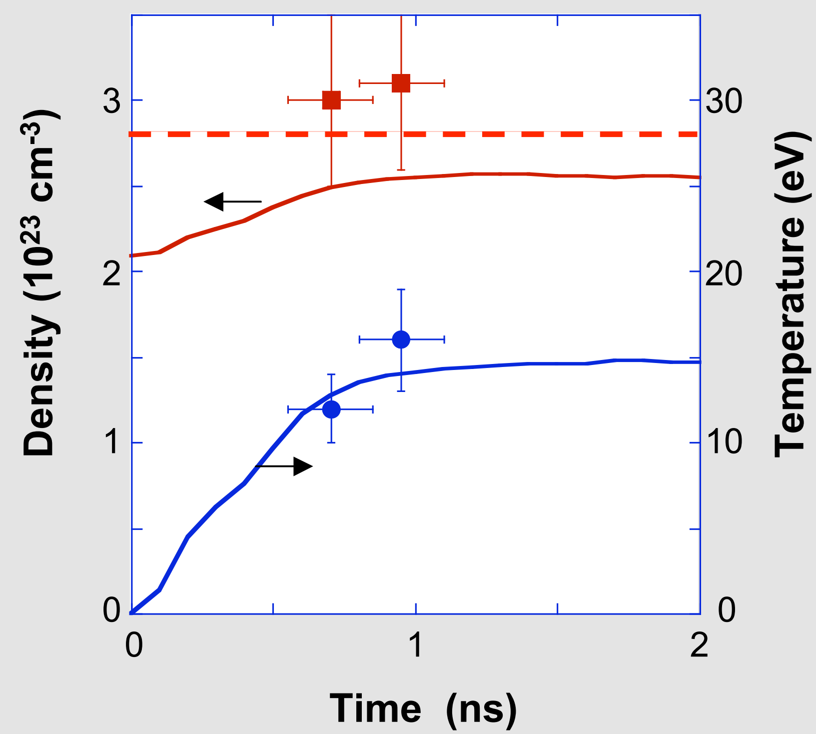

X-ray Thomson scattering has been shown to accurately characterize dense compressed matter

- Introduction
  - X-ray Thomson scattering from solid density plasmas
- Proof of principle experiments
  - Backscattering experiment
    - Compton scattering in dense plasmas
    - Accurate temperature diagnostics
  - Forward scattering experiment
    - First observation of Plasmons in Warm Dense Matter
    - Accurate density diagnostic
    - Importance of collisions
- **Compressed Matter**
  - **Compressibility and adiabat**
  - **Structure Factors**
  - **Coalescing shocks**
- Outlook and Conclusions

Compressed Be at 30 Mbar has been characterized with x-ray Thomson scattering

X-ray scattering on compressed Be has been performed at 90˚ and 25˚ scattering angle

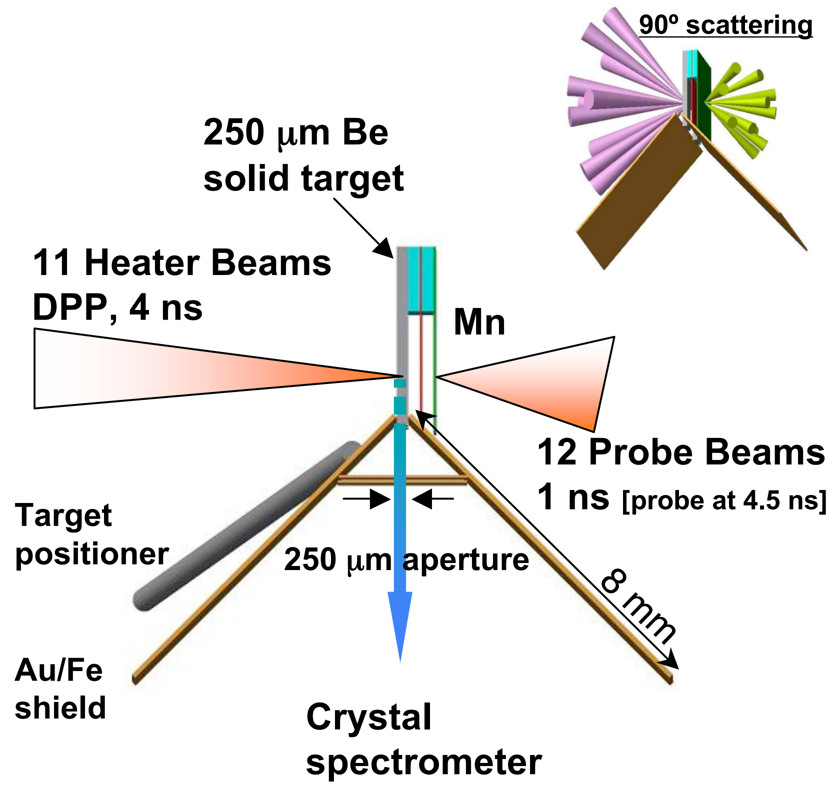

1-D Helios simulations indicate density of n_e = 7.5 x 10^{23} cm^{-3} [x3 compression]

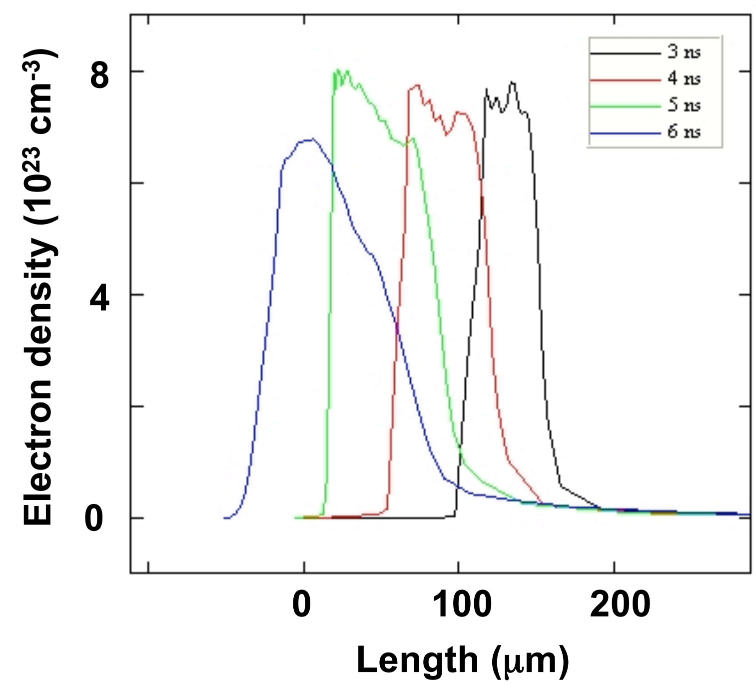

- A new Mn He-α backlighter at 6 keV was applied to penetrate through the dense compressed Be
- Disadvantage: double peaks from He-α and intercombination line

First X-ray Thomson scattering spectrum from compressed matter (Be)

The National Ignition Facility

Scattering data at 4.6 ns measure compressed matter density [E_F = 30 eV] and temperature

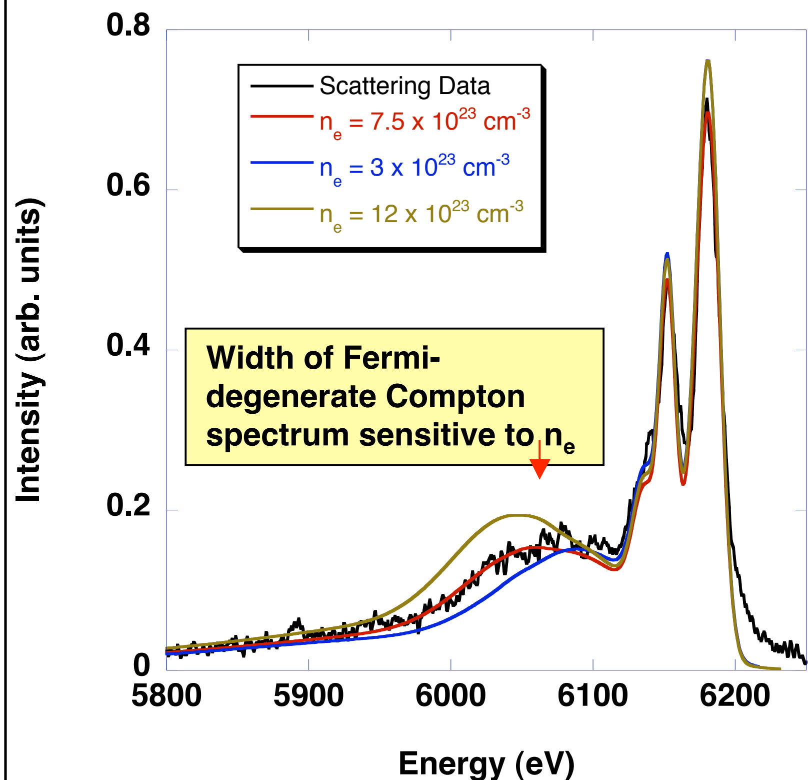

First X-ray Thomson scattering spectrum from compressed matter (Be)

The National Ignition Facility

Scattering data at 4.6 ns measure compressed matter density [E_F = 30 eV] and temperature

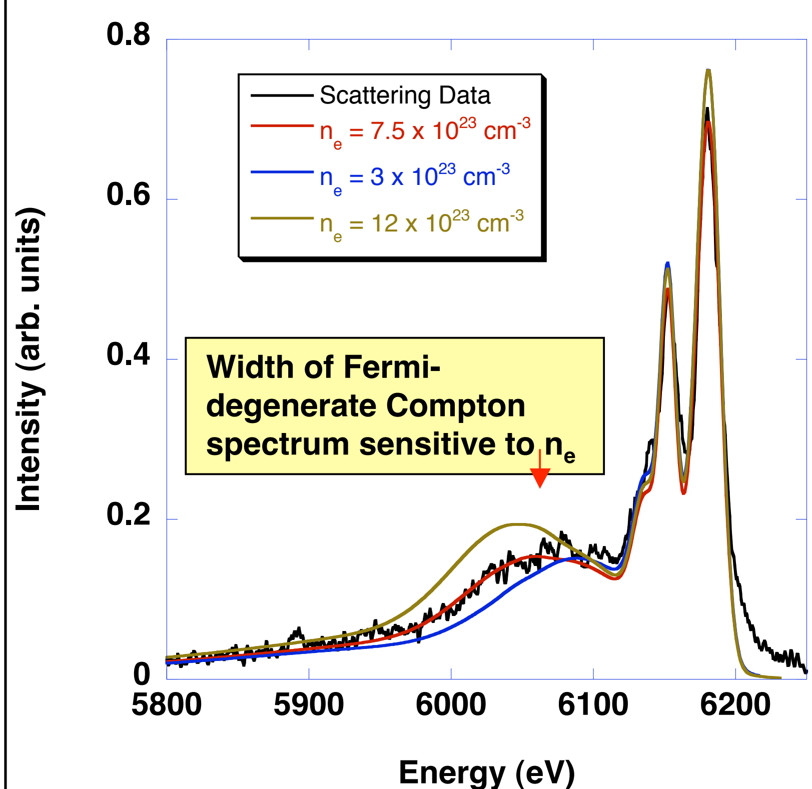

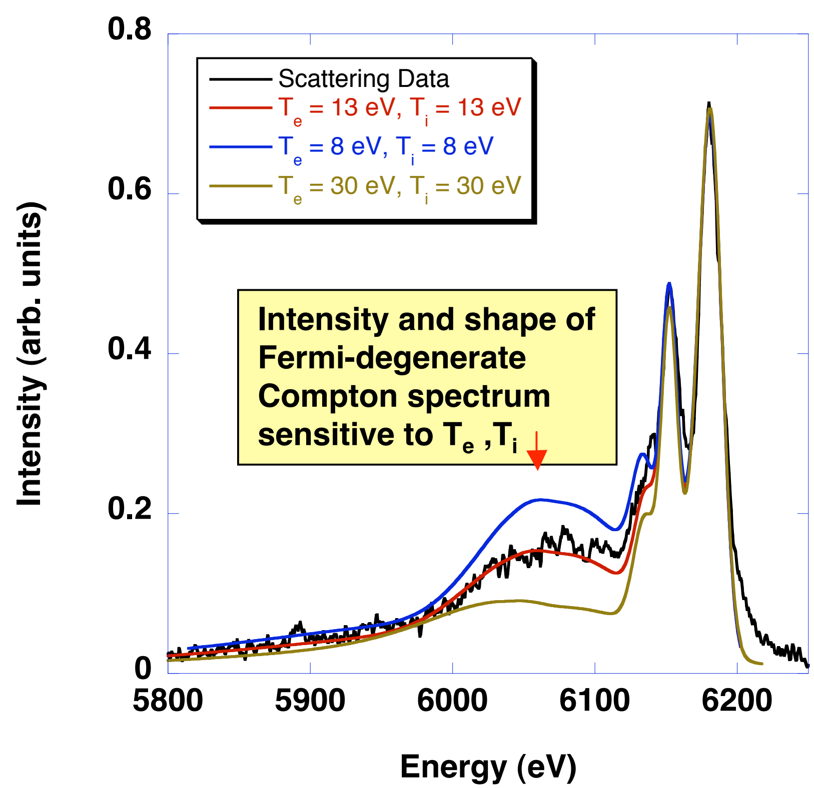

- 90˚ scatter, non-collective regime: $n_e = 7.5\times10^{23}$ cm^{-3}, T_e=13 eV, Z=2, α~0.5
- Consistent with simulations and forward scatter results
- First direct measure of increased Fermi energy and adiabat in laser-compressed matter

First X-ray Thomson scattering provides accurate characterization data

Scattering data at 4.6 ns measure compressed matter density [E_F = 30 eV] and temperature

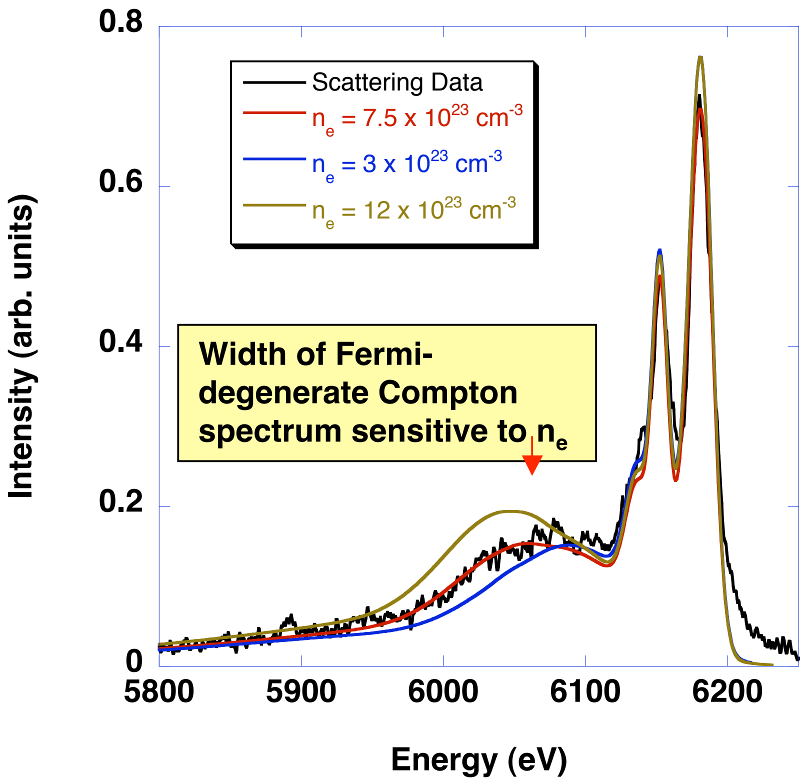

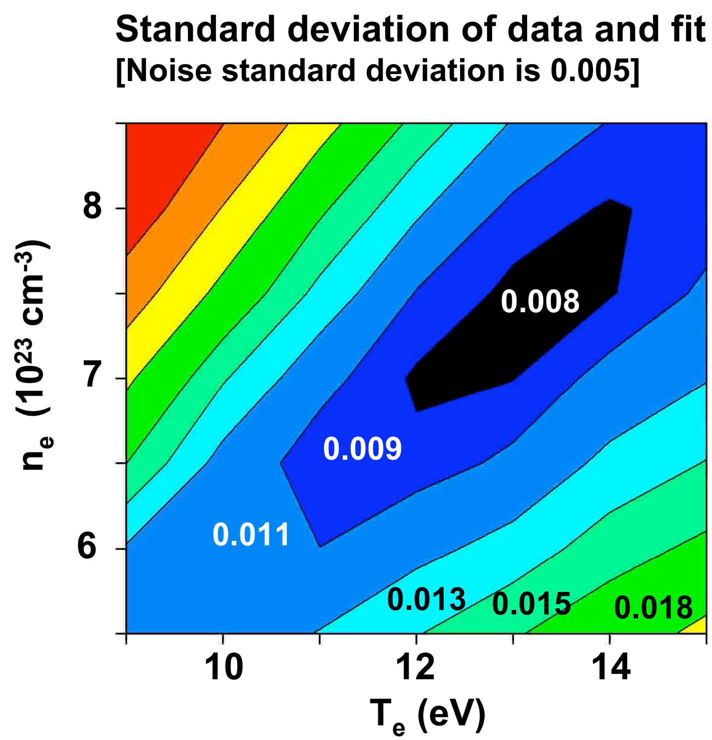

- Density and temperature are determined with an error bar of <10%
- High accuracy due to additional constraints on Z by the forward scattering data

Forward scattering data show plasmons at small energy shifts : collective regime , 25°

Scattering data at 4.4 ns measure compressed matter density [E_F = 30 eV]

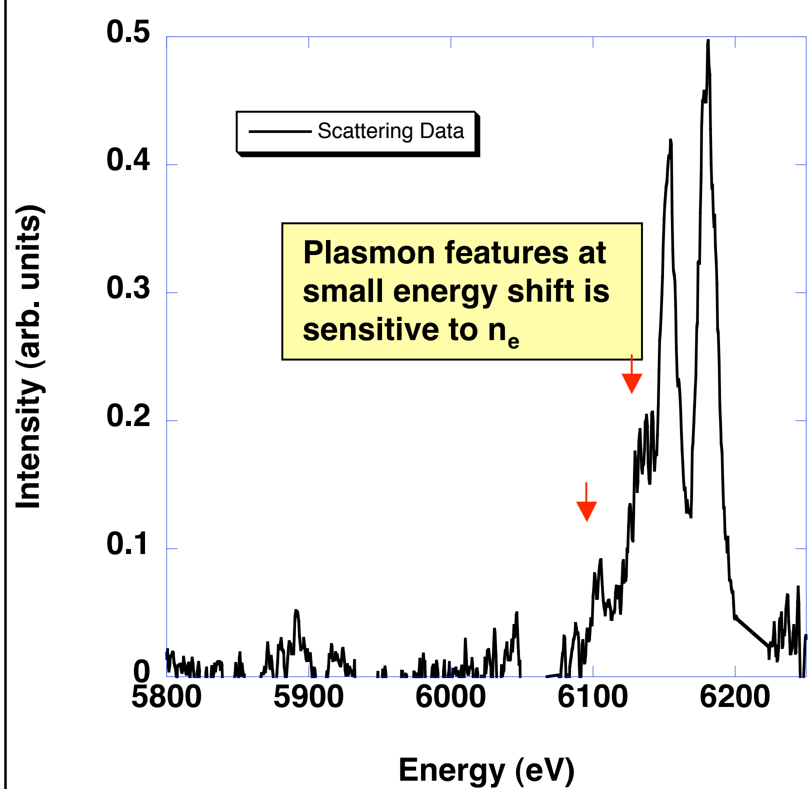

- Forward scatter: n_e=7.5x10^{23} cm^{-3}, T_e=12 eV, Z=2, α~1.6
- Forward scatter and backscatter results both provide compression of x3
- First direct measure of increased Fermi energy and adiabat in laser-compressed matter

Forward scattering data show plasmons at small energy shifts : collective regime , 25°

The National Ignition Facility

Scattering data at 4.4 ns measure compressed matter density [E_F = 30 eV]

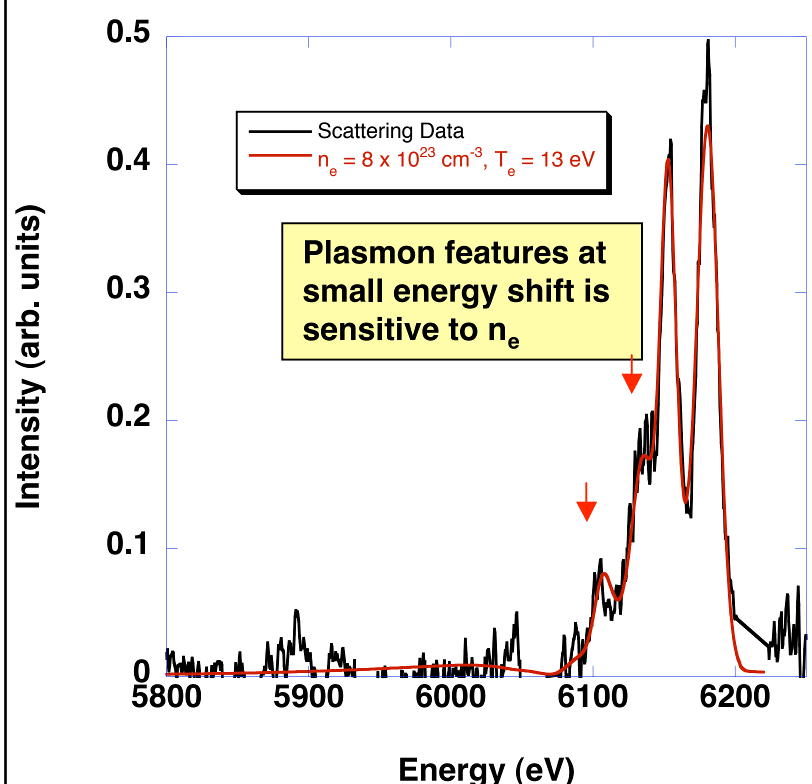

- Forward scatter: n_e=7.5x10^{23} cm^{-3}, T_e=13 eV, Z=2, α~1.6
- Forward scatter and backscatter results both provide compression of x3
- First direct measure of increased Fermi energy and adiabat in laser-compressed matter

Forward scattering data show plasmons at small energy shifts : collective regime , 25°

Scattering data at 4.4 ns measure compressed matter density [E_F = 30 eV]

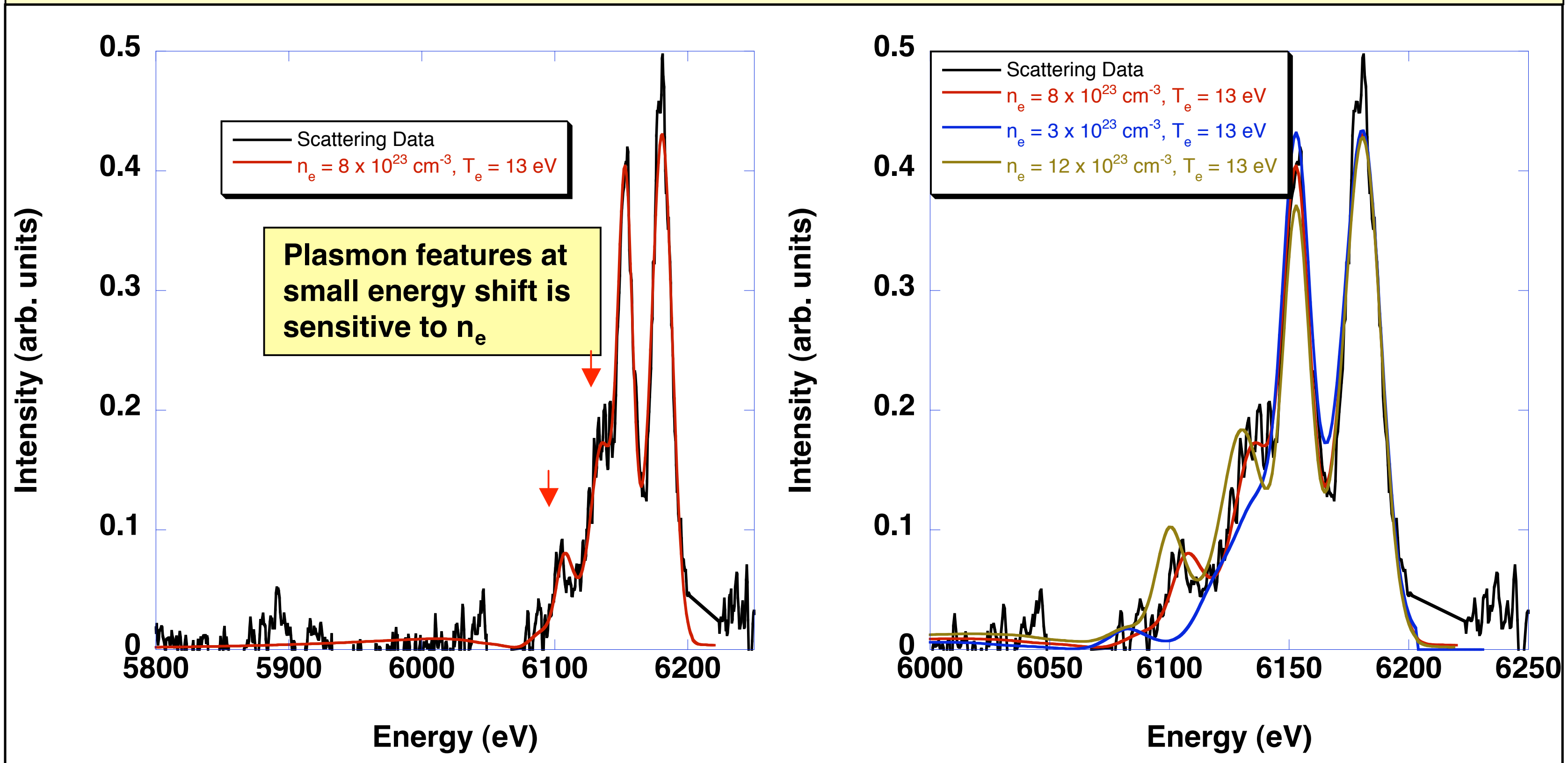

- First direct measure of increased Fermi energy, plasmons, and adiabat in laser-compressed matter
- Accurate characterization tool of laser-compressed matter

Scattering data will test hydrodynamic simulations of compressed matter conditions

Temperature and density for low and high pressure laser drive

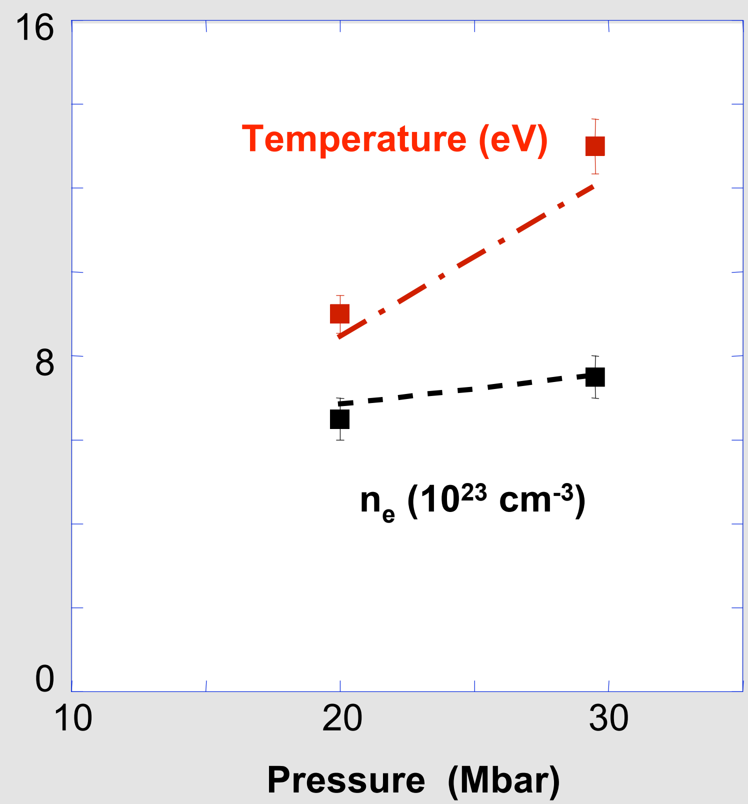

Preliminary comparison with HELIOS calculations (dashed lines) shows that temperature data are critical to test models

- **Electron density is only a weak function of pressure**
  - **Expected from Be Hugoniot data**
- **Temperature data**
  - **Include error from fits only**
  - **Sensitivity to structure factor calculations $S_{ii}(k)$ is being investigated**
  - **Experimental tests of structure factors**

Our experiments have tested the theory of structure factor calculations

The intensity of the elastic scattering depends on the structure factor - measure for different k: $\left|f_I(k)+q(k)\right|^2 S_{ii}(k,\omega)+\ldots$

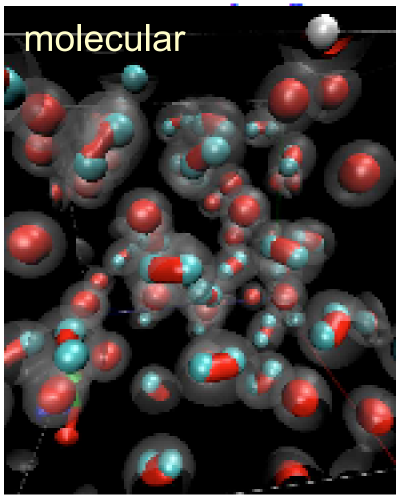

Hydrogen:
ρ=0.2 g/cc,
T =4000˚K

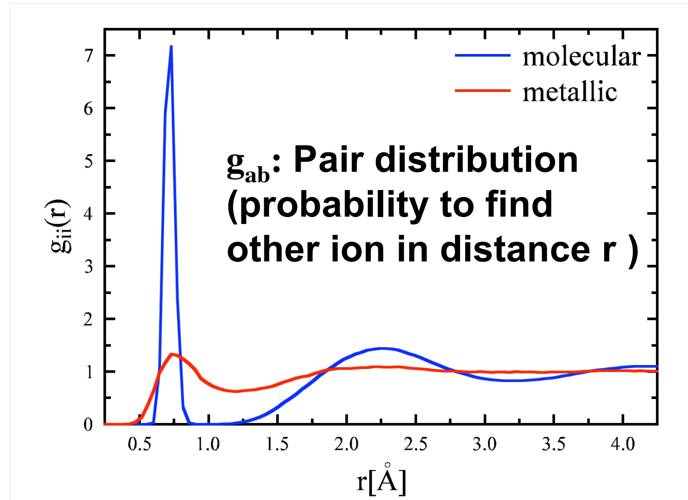

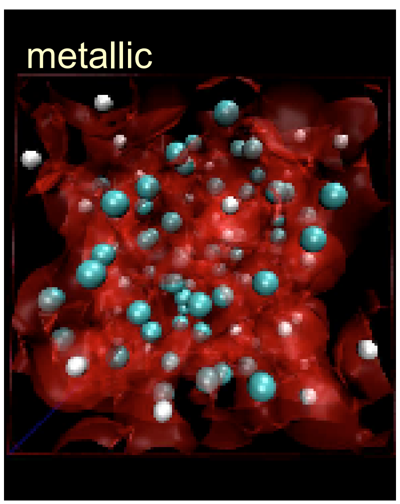

Hydrogen:
ρ=3.7 g/cc,
T =4000˚K

$$S_{ab}(k,\omega)=\delta_{ab}+\sqrt{n_a n_b}\int d\mathbf{r}\left[g_{ab}(r)-1\right]\exp(i\mathbf{kr})$$

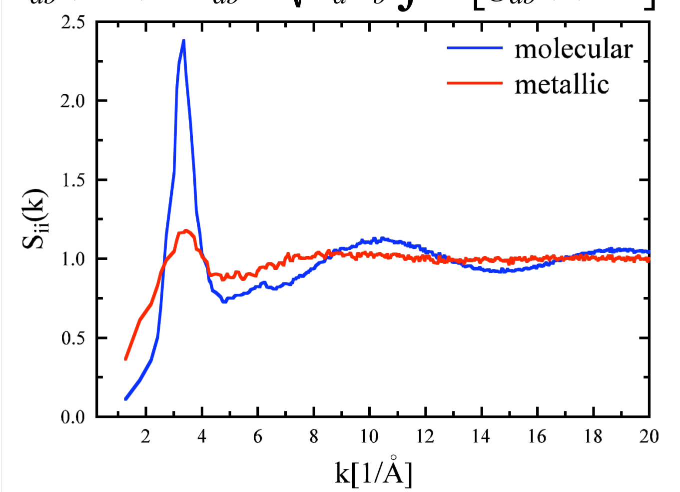

Measurements of the elastic x-ray scattering intensity for varying scattering angles allows testing structure factors

The National Ignition Facility

Ion Structure factor with DFT describes elastic scattering amplitude

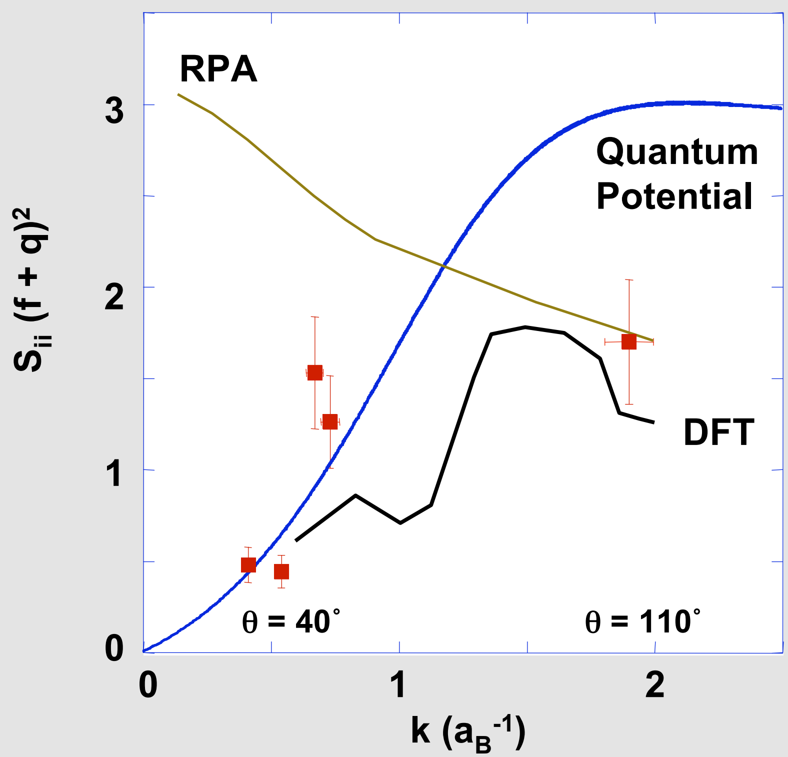

$$S(k,\omega) = \left| f_I(k) + q(k) \right|^2 S_{ii}(k,\omega) + \ldots$$

Ion feature

- **Data for**
  - $T_e = T_i = 12$ eV
  - $n_e = 3 \times 10^{23}$ cm^{-3}
- **For θ=40˚ and θ=110˚ the elastic scattering amplitude is absolutely determined from the inelastic scattering feature**
- **For k = 2 we have**
  - Non-collective scatter
  - q approaches zero
  - S_{ii} approaches one

- **Density Functional Theory (DFT) has validated weak electron-ion interactions for small k as predicted by quantum potentials**

The first inelastic Thomson scattering measurements on a medium-sized laser have been successful on Titan [300 J]

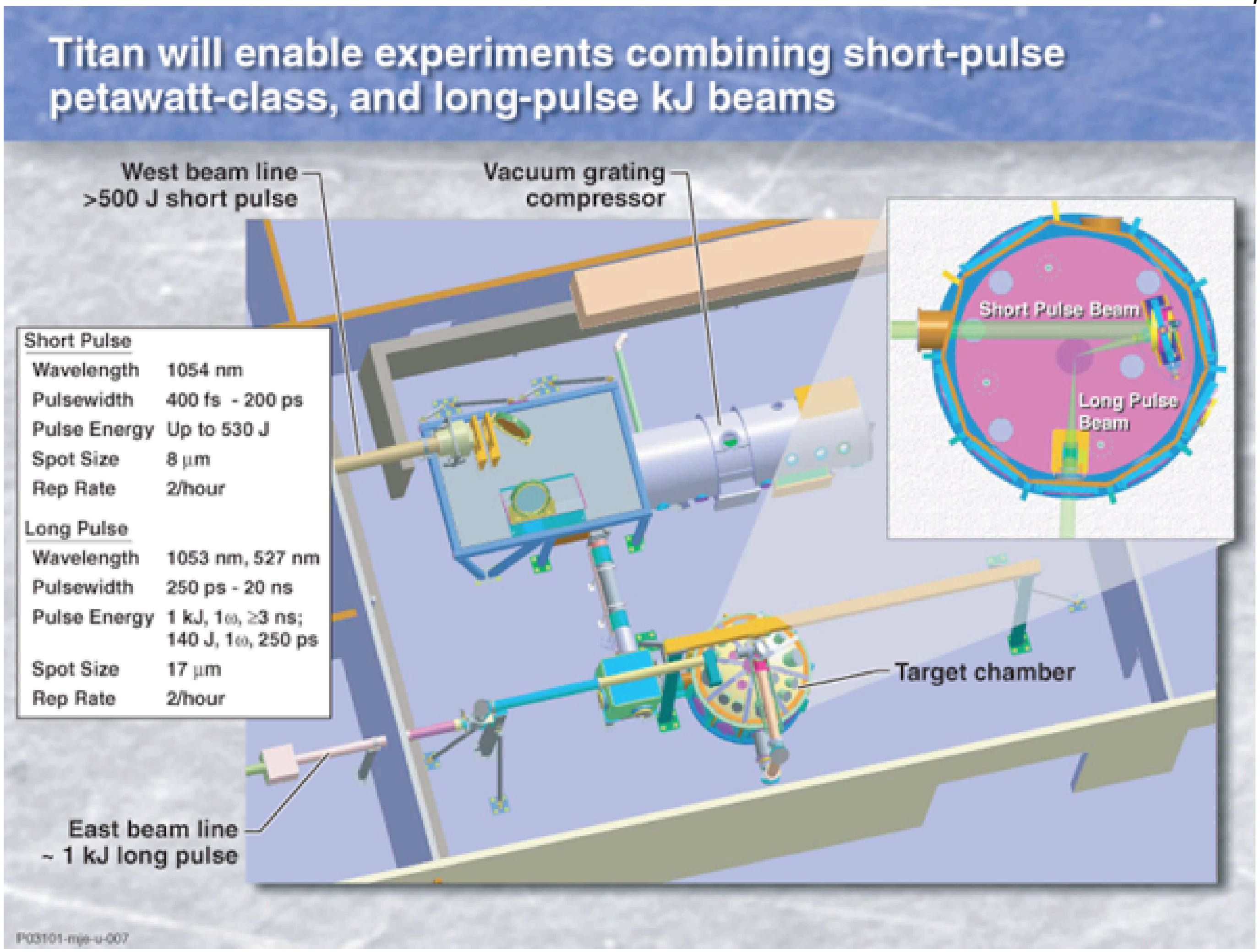

Pump-probe experiments with K-alpha x-rays allowing to probe with 10 ps temporal resolution

K-α Compton scattering on the LLNL's Titan laser measures temperature in shock-compressed matter with 10 ps resolution

The National Ignition Facility

K-α x-rays at 4.5 keV have been applied to scatter on dense compressed LiH

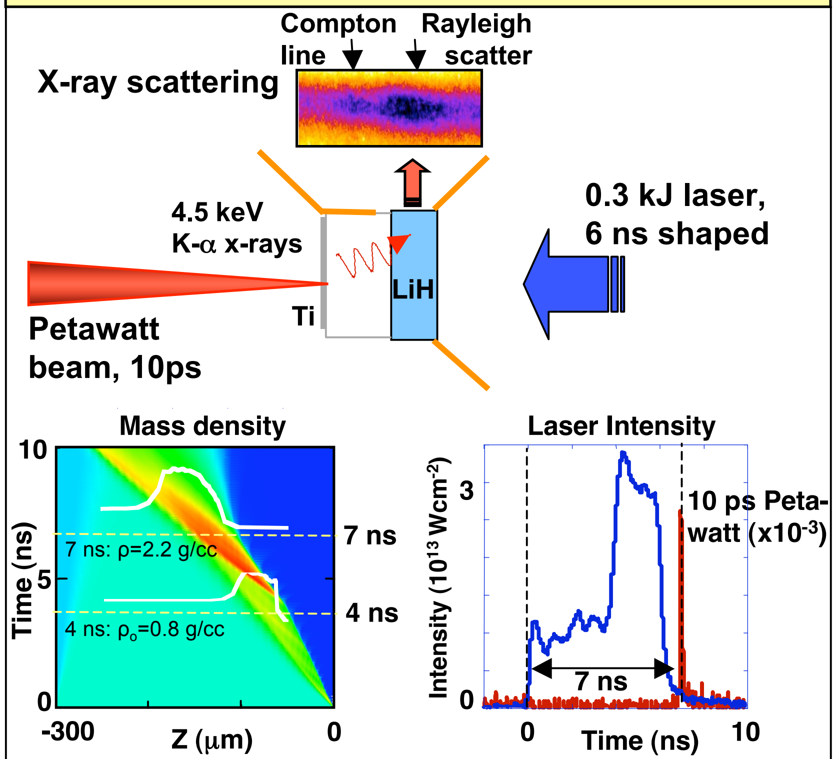

Shaped drive launches two shocks that coalesce at 7ns with $n_e = 1.7 \times 10^{23}$ cm^{-3}

Compton scattering determines the temperature of T = 2.8 eV (± 20%)

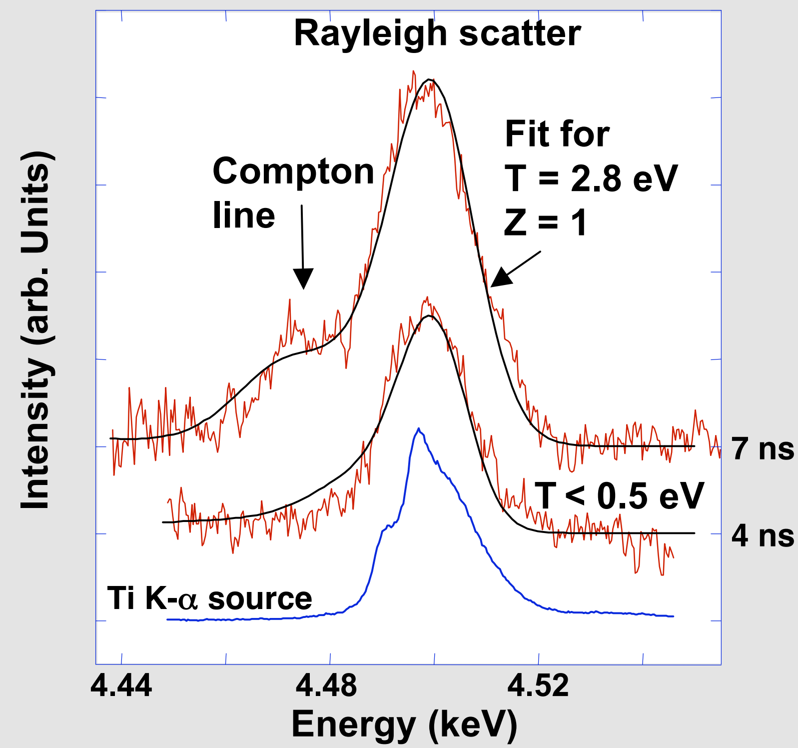

First measurement in coalescing shocks shows 30% larger T values than simulations

- **Compton scattering on NIF will characterize shock-compressed matter with ultrahigh temporal resolution of 10 ps**

University Relations Program

A sensitivity analysis shows that single-shot scattering data determine temperatures with an error bar of 20%

The National Ignition Facility

The intensity of the inelastic (Compton) scattering features is temperature sensitive

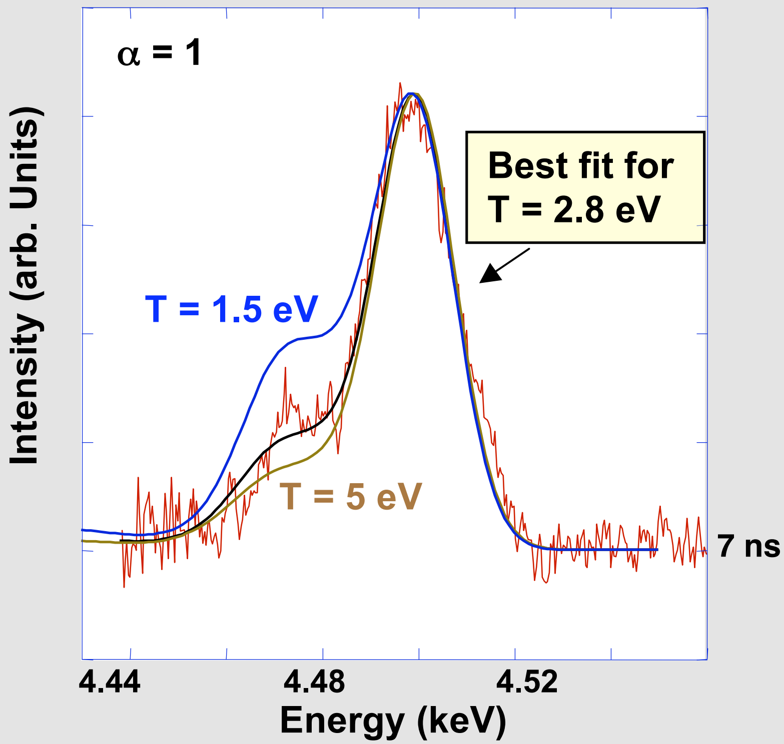

First measurement in coalescing shocks shows T = 2.8 eV (analysis assumes $T_e = T_i$)

- K-α scattering has been developed to provide accurate characterization of dense matter
- Compressed Matter experiment
  - First successful experiments on compressed LiH
  - Data from Titan are of sufficient quality to test radiation-hydrodynamic modeling
- Density is constraint by the width of the Compton feature
  - Consistent with x 2.8 compression

University Relations Program

The Thomson scattering data test hydrodynamic modeling of the temperature evolution in shocked matter

Coalescing shocks are an effective heating mechanism

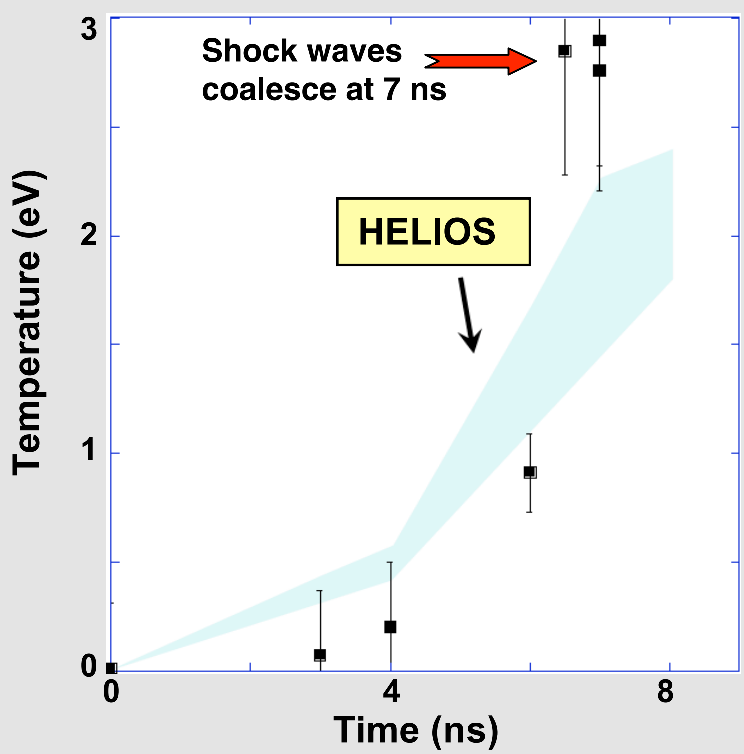

Range of temperatures from HELIOS is due to variations within the scattering volume

- **Temperatures in hydrodynamic modeling is sensitive to**
  - Equation of state
  - Radiation transport
  - Heat transport

- **Demonstrates technique to characterize NIF Fusion Capsules**
  - A sequence of four shocks will have to be accurately timed before compression and burn

X-ray Thomson scattering has been shown to accurately characterize dense compressed matter

- Introduction
  - X-ray Thomson scattering from solid density plasmas
- Proof of principle experiments
  - Backscattering experiment
    - Compton scattering in dense plasmas
    - Accurate temperature diagnostics
  - Forward scattering experiment
    - First observation of Plasmons in Warm Dense Matter
    - Accurate density diagnostic
    - Importance of collisions
- Compressed Matter
  - Compressibility and adiabat
  - Structure Factors
  - Coalescing shocks
- **Outlook and Conclusions**

X-ray scattering measures Compton and Plasmon features directly providing T_e/T_F

Radiation-hydrodynamic simulations of NIF implosions

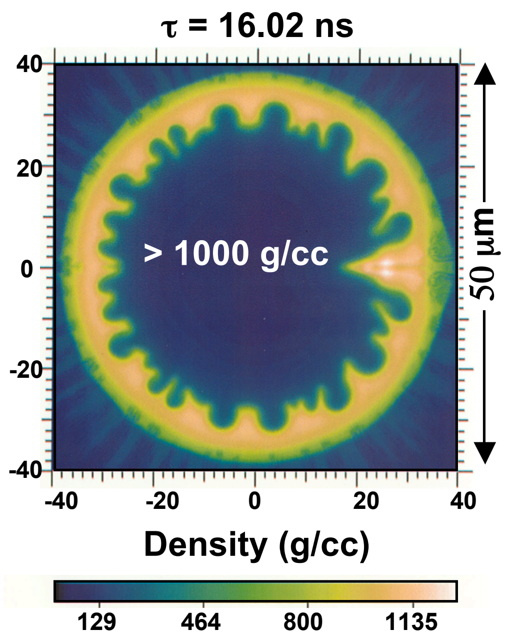

Compressed fuel at high density (up to 1000 g/cc), efficient at low T_e: T_e/T_F<1

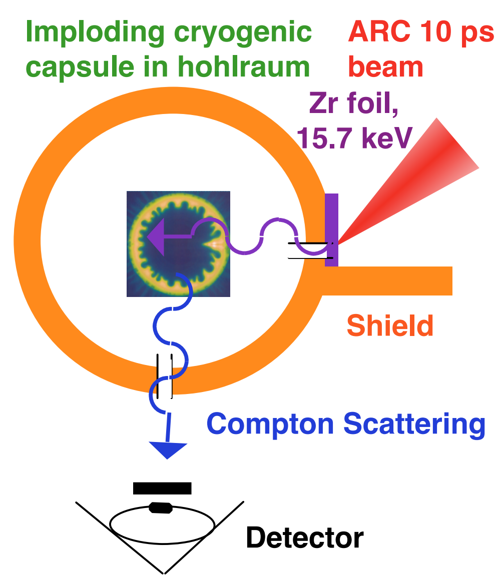

X-ray scattering spectrum from implosion calculated by post-processing HYDRA

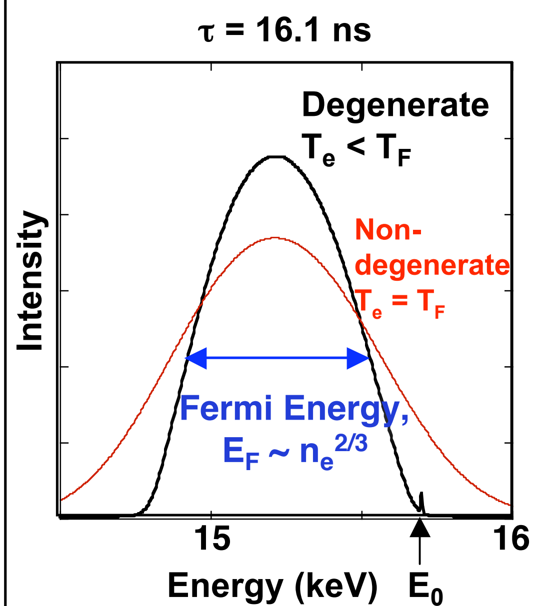

- **Goal: Characterize shock-compressed matter**
  - Measure temperature and density with ultrahigh temporal resolution
  - Compressibility, demonstrate n_e measurement of up 1000 g/cc

Applications

Calculations for Free Electron Lasers indicate accurate characterization of the role of collisions

The National Ignition Facility

Scattering spectra show Plasmon intensity determined by detailed balance, $I \sim e^{-h\nu/kT_e}$

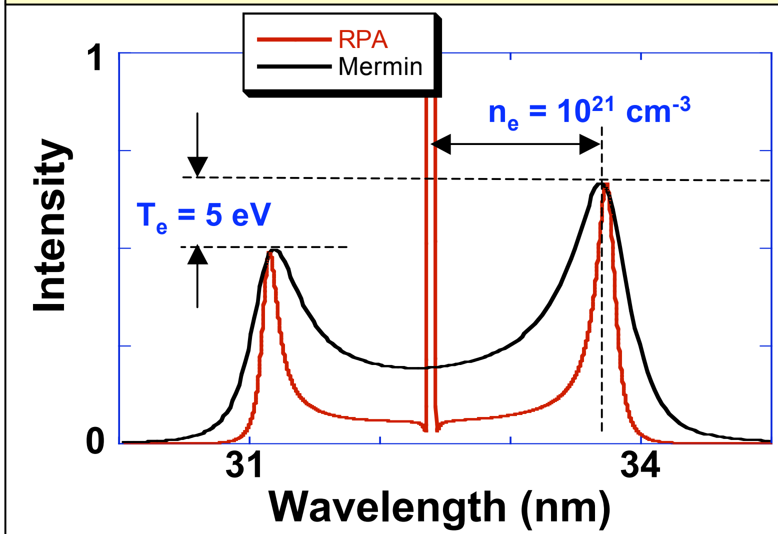

VUV-FEL pulse can provide > 10^{12} photons for Thomson scattering experiments

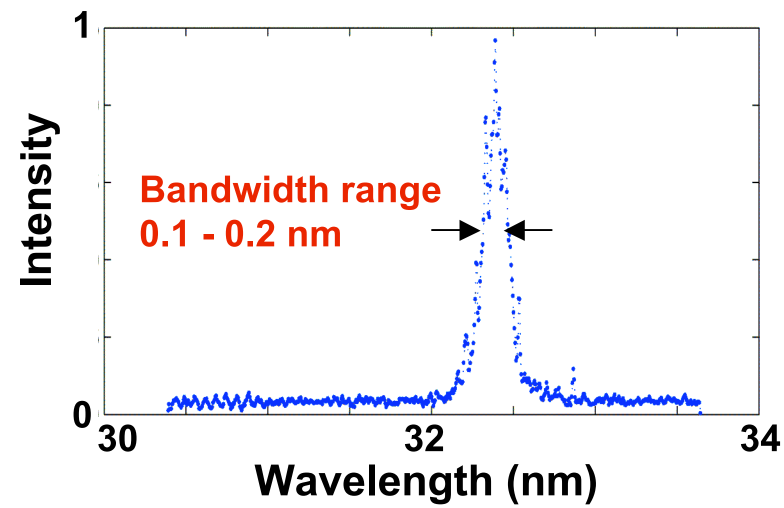

Undulator at VUV-FEL, DESY

Free Electron Laser beam;
Example: 32 nm, 20 fs, 50 μJ

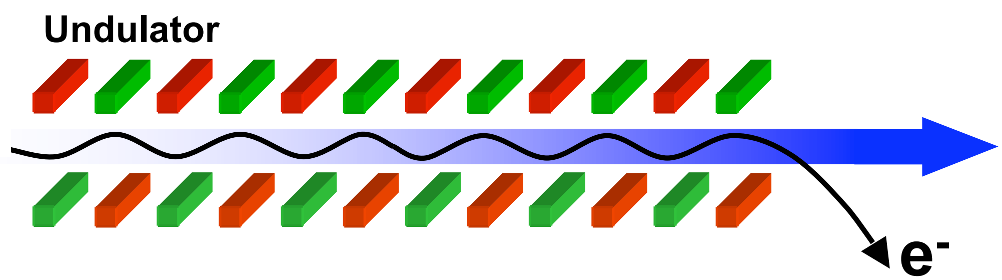

Conclusions

The National Ignition Facility

- X-ray Thomson scattering has been developed for accurate measurements of temperatures and densities in dense matter

- Back scatter
  - Measures velocity distribution function: electron temperature T_e
  - Elastic (Rayleigh) scattering: Z_{free} diagnostics [n_e in isochorically heated matter]

- Forward scatter
  - First observation of Plasmons in warm dense matter: electron density n_e
  - Future experiments may allow accurate measurement of collisions and conductivity

- Compressed Matter experiments
  - First successful experiments on compressed Be
  - Titan coalescing shocks
  - Technique to characterize NIF Fusion Capsules
  - Technique to characterize high energy density physics regime [equation of state, phase transitions, metallic fluids]

The first experimental evidence for the Plasma Phase transition have been published this year by Fortov et al.

The fact that the multiple densities exist for the same pressure would indicate a phase transition; x-ray Thomson scattering can directly determine its existence